

INVESTIGATION OF THE LIMITS OF INERTIAL SUPPORT
IMPLEMENTATION IN VARIABLE SPEED WIND TURBINES AND THE
EFFECTS OF SYNTHETIC INERTIA IN POWER SYSTEM FREQUENCY
STABILITY

A THESIS SUBMITTED TO
THE GRADUATE SCHOOL OF NATURAL AND APPLIED SCIENCES
OF
MIDDLE EAST TECHNICAL UNIVERSITY

BY

ERENCAN DUYMAZ

IN PARTIAL FULFILLMENT OF THE REQUIREMENTS
FOR
THE DEGREE OF MASTER OF SCIENCE
IN
ELECTRICAL AND ELECTRONICS ENGINEERING

DECEMBER 2018

Approval of the thesis:

**INVESTIGATION OF THE LIMITS OF INERTIAL SUPPORT
IMPLEMENTATION IN VARIABLE SPEED WIND TURBINES AND THE
EFFECTS OF SYNTHETIC INERTIA IN POWER SYSTEM FREQUENCY
STABILITY**

submitted by **Erencan Duymaz** in partial fulfillment of the requirements for the degree of **Master of Science in Electrical and Electronics Engineering Department, Middle East Technical University** by,

Prof. Dr. Gülbilin Dural Ünver _____
Dean, Graduate School of **Natural and Applied Sciences**

Prof. Dr. Bölüm Başkanı _____
Head of Department, **Electrical and Electronics Engineering**

Ozan KEYSAN _____
Supervisor, **Department of Electrical and Electronics Engineering, METU**

Examining Committee Members:

Prof. Dr. Jüri _____
JüriBölüm, METU

Prof. Dr. Jüri _____
JüriBölüm, METU

Prof. Dr. Jüri _____
JüriBölüm, METU

Assoc. Prof. Dr. Jüri _____
JüriBölüm, METU

Assist. Prof. Dr. Jüri _____
JüriBölüm, Ankara University

Date: _____

I hereby declare that all information in this document has been obtained and presented in accordance with academic rules and ethical conduct. I also declare that, as required by these rules and conduct, I have fully cited and referenced all material and results that are not original to this work.

Name, Last Name: Erencan Duymaz

Signature : 

ABSTRACT

INVESTIGATION OF THE LIMITS OF INERTIAL SUPPORT IMPLEMENTATION IN VARIABLE SPEED WIND TURBINES AND THE EFFECTS OF SYNTHETIC INERTIA IN POWER SYSTEM FREQUENCY STABILITY

DUYMAZ, ERENÇAN

M.S., Department of Electrical and Electronics Engineering

Supervisor : Ozan KEYSAN

December 2018, 91 pages

The share of renewable energy systems in the installed capacity increases dramatically. Research shows that increase in the renewable energy percentage brings power system stability problems due to the decrease in the grid aggregated inertia. To prevent the decrease in the grid inertia, renewable energy systems should possess the inertial support capability that is the inherited behaviour of the conventional synchronous generators. Especially, variable speed wind turbines are able to provide additional amount of active power in the frequency disturbances by extracting the kinetic energy stored in the turbine and generator inertia. In this study, the inertial support implementation is studied for variable speed wind turbines with a full-scale power electronics. To increase the active power as desired, Machine Side Converter is modified with an additional control loop. In the first part of the thesis, active power of the wind turbine is increased to the limits and the maximum achievable active power is found out to be restricted by the wind speed. It is also found that the wind turbine can increase its output power by 40% of rated power in the low and medium

wind speeds. Moreover, even though the high speed scenarios gives limited increased power, it does not require any speed recovery state. The probability of different wind speeds and the inertial supports are found according to the wind speed measurement taken from field. In the second part of the thesis, the synthetic inertia implementation is presented by the provision of inertial support proportional to rate of change of frequency. The effect of the implementation in the P.M.Anderson test case is observed for different inertia constants. It is discovered that the effect of renewable penetration in the frequency stability is negligible when the synchronous generators are kept in the operation. Nonetheless, frequency stability in the test system gets more vulnerable with renewable energy penetration when the conventional generators are decommissioned by the economical concerns. In this case, the synthetic inertia implementation with different inertia constants possess the ability to lower RoCoF following a frequency disturbance.

Keywords: Power System Frequency Stability, Inertial Support, Synthetic Inertia, Virtual Inertia, Renewable Energy

ÖZ

DEĞİŞKEN HIZLI RÜZGAR TÜRBİNLERİİNDE ATALET DESTEĞİNİN SINIRLARININ İNCELENMESİ VE YAPAY ATALET DESTEĞİNİN GÜÇ SİSTEMLERİ FREKANS STABİLİTESİNE ETKİLERİ

DUYMAZ, ERENCAN

Yüksek Lisans, Elektrik ve Elektronik Mühendisliği Bölümü

Tez Yöneticisi : Ozan KEYSAN

Aralık 2018 , 91 sayfa

Kurulu güçteki yenilenebilir enerji oranı önemli ölçüde artmaktadır. Araştırmalara göre yenilenebilir enerji oranındaki artış şebekenin toplu ataletindeki düşüşten kaynaklanan güç sistemleri stabilite sorunlarını da beraberinde getirmektedir. Şebeke ataletindeki bu düşüşü engellemek için, yenilenebilir enerji sistemleri konvansiyonel senkron makinelerin doğuştan sahip olduğu atalet desteği yeteneğine sahip olmalıdır. Özellikle, değişken hızlı rüzgar türbinleri frekans bozunu anlarında, türbin ve generatör ataletinde depolanmış hareket enerjisini soğurarak şebekeye fazla güç basabilir. Bu çalışmada, tam ölçek güç elektronikli değişken hızlı rüzgar türbinleri için atalet desteği uygulanmıştır. Aktif gücün istenildiği gibi artırılabilmek için Makine Tarafı Kontrolcüsüne kontrol döngüsü eklenmiştir. Bu tez çalışmasının ilk kısmında, rüzgar türbinin aktif gücü sınır noktalarına kadar artırılmıştır ve ulaşılabilir maksimum gücün rüzgar hızıyla kısıtlandığı gözlenmiştir. Ayrıca, düşük ve orta rüzgar hızlarında rüzgar türbininin aktif gücünü nominal gücünün %40'ı oranda arttırbildiği gözlenen bulgular arasındadır. Bunun yanında, yüksek rüzgar senaryolarında sınırlı güç artışı

gözlense de, generatör hızının toparlanma evresine gerek duymadığı gözlenmiştir. Sahadan alınan rüzgar hızı verilerine göre değişik rüzgar hızı ve atalet desteklerinin olma olasılıkları da hesaplanmıştır. Tezin ikinci kısmında, frekansın değişim hızıyla ortantılı atalet desteği uygulayarak yapay atalet desteği uygulanmıştır. Bu uygulamanın etkileri, değişik atalet sabitleri ile P.M. Abderson test düzeneğinde gözlenmiştir. Buna göre, konvansiyonel senkron makineler operasyonda olduğu sürece, yenilenebilir enerji penetrasyonun frekans stabilitesine olan etkisinin ihmali edilebilir düzeyde olduğu görülmüştür. Ancak, generatörlerin ekonomik kaygılarla operasyondan alındığı durumlarda, yenilenebilir enerji penetrasyonun frekans stabilitesini zayıflattığı gözlenmiştir. Bu durumlar, değişik atalet sabitleriyle uygulanabilen yapay ataletin frekans bozumalarında sistemin frekans değişim hızını azalttığı sonucuna varılmıştır.

Anahtar Kelimeler: Güç Sistemleri Frekans Stabilitesi, Atalet Desteği, Yapay Atalet, Sanal Atalet, Yenilebilir Enerji

To my precious mom...

ACKNOWLEDGMENTS

Teşekkür edilecekler

TABLE OF CONTENTS

ABSTRACT	v
ÖZ	vii
ACKNOWLEDGMENTS	x
TABLE OF CONTENTS	xi
LIST OF TABLES	xv
LIST OF FIGURES	xvi
LIST OF ABBREVIATIONS	xx
LIST OF SYMBOLS	xxi
CHAPTERS	
1 INTRODUCTION	1
1.1 Global Renewable Energy Status	1
1.1.1 EU 2020 Goals	3
1.1.2 Wind Energy Status	4
1.2 Global Renewable Energy Future	5
1.3 Renewable Energy Problems	6
1.4 Literature Review	10
1.5 Thesis Motivation	11

1.6	Thesis Outline	12
2	POWER SYSTEM FREQUENCY STABILITY	15
2.1	Synchronous Generator and Synchronous Speed	15
2.2	Swing Equation	16
2.3	Frequency in Power Systems	17
2.3.1	Primary Frequency Control	18
2.3.2	Secondary and Tertiary Control	19
3	WIND TURBINE MODELLING	21
3.1	Variable Speed PMSG Wind Turbines	21
3.1.1	Aerodynamic Model	22
3.1.1.1	Maximum Power Point Tracking Algorithms	23
3.1.1.2	Pitch Angle Control	24
3.1.2	Gearbox	26
3.1.3	Permanent Magnet Synchronous Generator	27
3.1.4	Machine Side Converter	28
3.1.5	Grid Side Converter	29
3.2	Synthetic Inertia Implementation	32
3.2.1	Synthetic Inertia Activation Schemes	33
3.2.2	Source of the Inertial Support	34
4	INVESTIGATION OF INERTIAL SUPPORT PRACTICAL LIMITS	37
4.1	Inertial Support Limits	37
4.2	Fast Inertial Support Under Different Wind Speeds	40

4.2.1	Low Wind Scenario	40
4.2.1.1	Fast Inertial Support Limit in Low Wind Scenario	40
4.2.1.2	Moderate Fast Inertial Support for in Low Wind Scenario	43
4.2.2	Medium Wind Scenario	45
4.2.2.1	Fast Inertial Support Limit in Medium Wind Scenario	46
4.2.2.2	Moderate Fast Inertial Support for in Medium Wind Scenario	47
4.2.3	High Wind Scenario	49
4.2.3.1	Fast Inertial Support Limit in High Wind Scenario	50
4.2.3.2	Moderate Inertial Support Limit in High Wind Scenario	52
4.3	Probabilistic Approach for Fast Inertial Support	54
5	EFFECTS OF SYNTHETIC INERTIA IMPLEMENTATION	57
5.1	P.M.Anderson 9 Bus Test Case	57
5.1.1	System Properties	57
5.1.2	Load Flow Analysis for Base Case	59
5.1.3	Base Case Frequency Response for Additional Load Connection	59
5.2	Modified Case	61
5.2.1	Load Flow Analysis for Modified Case	63
5.2.2	Modified Case Frequency Response for Additional Load Connection	63
5.3	Decommissioned Case	64

5.3.1	Load Flow Analysis for Decommissioned Case	66
5.3.2	Decommissioned Case Frequency Response for Ad- ditional Load Connection	67
5.4	Modified Case with Synthetic Inertia	67
5.5	Decommissioned Case with Synthetic Inertia	70
5.6	Comparison of the Synthetic Inertia and Fast Inertial Support	71
6	EVALUATION OF FAST INERTIAL RESPONSE AND SYNTHETIC INERTIA IMPLEMENTATION	75
6.1	Fast Inertial Support	76
6.2	Synthetic Inertia Implementation	77
6.3	FUTURE WORK	79
	REFERENCES	81
A	WIND TURBINE PARAMETERS	87
B	P.M. ANDERSON TEST CASE PROPERTIES	89

LIST OF TABLES

TABLES

Table 1.1 Comparison of Different Type of Generators for Inertial Response Behaviour	9
Table 5.1 Generator Properties of Test System	58
Table 5.2 Load Properties of Test System	58
Table 5.3 Load Flow Results in Base Case	59
Table 5.4 System Dynamical Properties	60
Table 5.5 Load Flow Results for Modified Case	63
Table 5.6 System Dynamical Properties	66
Table 5.7 Load Flow Results for Decommissioned Case	66
Table A.1 Wind Turbine Parameters Used in the Thesis	87
Table B.1 Load Data of the P.M. Anderson Test System	89
Table B.2 Line Data of the P.M. Anderson Test System	89
Table B.3 Generator Data of the P.M. Anderson Test System	90
Table B.4 Transformer Data of the P.M. Anderson Test System	91

LIST OF FIGURES

FIGURES

Figure 1.1 Installed Renewable Energy Capacity of Leading Countries	1
Figure 1.2 Renewable Energy Production of Leading Countries	2
Figure 1.3 Average Renewable Energy Generation per MW in 2016	3
Figure 1.4 Renewable Targets of EU Member States [1]	4
Figure 1.5 Wind Power Capacity of Leading Countries in 2016	5
Figure 1.6 Wind Power Production of Leading Countries in 2016	6
Figure 1.7 Wind Power Production of Leading Countries in 2016	7
Figure 1.8 Renewable energy share in total energy consumption by EU for 2015, 2020 targets and 2030 potential according to REmap [2]	7
Figure 1.9 Renewable energy shares for 2010, 2030 Reference Case and 2030REmap [3]	8
Figure 2.1 Damper windings in a synchronous generator [4]	15
Figure 2.2 Frequency behaviour in electric grid with the water level in a con- tainer analogy [5]	18
Figure 3.1 Variable Speed Geared Wind Turbine Model	21
Figure 3.2 Power Coefficient Variation with Tip Speed Ratio under Zero Pitch Angle	23
Figure 3.3 Power Coefficient Variation for Two Different Pitch Angle	25

Figure 3.4 Pitch Angle Control Diagram	25
Figure 3.5 Power Coefficient Varion for GE 2.75-103	26
Figure 3.6 Gearbox Modelling	27
Figure 3.7 Machine Side Control Diagram	29
Figure 3.8 Grid Side Control Diagram	30
Figure 3.9 Variation of the Active Power of the Wind Turbine	31
Figure 3.10 Modified MSC for Inertial Support	32
Figure 4.1 Active Power Flow Diagram	37
Figure 4.2 Increase in the Active Power Output for Varying Wind Speeds . . .	39
Figure 4.3 Fast Inertial Support Active Power Limit for Low Wind Scenario .	41
Figure 4.4 Generator and Turbine Power and Generator Speed for Low Wind Speed Limit Case	42
Figure 4.5 Variation of DC-bus Voltage for Low Wind Speed Limit Case . . .	42
Figure 4.6 Active Power Output of the Wind Turbine for Low Wind Scenario .	43
Figure 4.7 Generator Speeds of the Wind Turbine for Low Wind Scenario . . .	44
Figure 4.8 Turbine Torque, Generator Speed and Torque for 5 Seconds Sup- port under Low Wind Speed	44
Figure 4.9 Turbine Torque, Generator Speed and Torque for 20 Seconds Sup- port under Low Wind Speed	45
Figure 4.10 DC-Link Voltage for 20 Seconds Support in Low Wind Speed . . .	45
Figure 4.11 Fast Inertial Support Active Power Limit for Medium Wind Scenario	46
Figure 4.12 Generator and Turbine Power and Generator Speed for Medium Wind Speed Limit Case	46

Figure 4.13 Variation of DC-bus Voltage for Medium Wind Speed Limit Case	47
Figure 4.14 Active Power Output of the Wind Turbine for Medium Wind Scenario	48
Figure 4.15 Generator Speed, Generator and Turbine Torques for Medium Wind Scenario for 20 Seconds Support	48
Figure 4.16 DC-Link Voltage for 20 Seconds Support in Medium Wind Speed	49
Figure 4.17 Fast Inertial Support Active Power Limit for High Wind Scenario	50
Figure 4.18 Turbine and Generator Powers, Generator Speed and Pitch Angle for High Wind Limit Scenario	51
Figure 4.19 Variation of the DC-bus Voltage for High Wind Limit Scenario	51
Figure 4.20 Active Power Output of the Wind Turbine for High Wind Scenario	52
Figure 4.21 Pitch Angle, Generator Speed, Generator and Turbine Torques for High Wind Scenario for 20 Seconds Support	53
Figure 4.22 Probability Density Function of Measured Wind Speeds	54
Figure 4.23 Cumulative Distribution Function of Measured Wind Speeds	55
Figure 4.24 Distribution of Fast Inertial Support	56
 Figure 5.1 P.M.Anderson Test Case	58
Figure 5.2 Location of the Additional Load	60
Figure 5.3 Generator Frequencies for 10% Load Connection	61
Figure 5.4 Frequencies in Generator 1, Load A and Load B	62
Figure 5.5 Modified System Single Line Diagram	62
Figure 5.6 Comparison of Base Case and Modified Case Frequencies	64
Figure 5.7 Comparison of Base Case and Modified Case Frequencies	65
Figure 5.8 Decommissioned Case Sinle Line Diagram	65

Figure 5.9 Comparison of Base Case,Modified Case and Decommissioned Case Frequency Responses	67
Figure 5.10 Comparison of Base Case,Modified Case and Decommissioned Case RoCoFs	68
Figure 5.11 Emulation of the Different Inertia Constants for the Modified Case	68
Figure 5.12 RoCoF of the Different Inertia Constants for the Modified Case . .	69
Figure 5.13 RoCoF of the Different Inertia Constants for the Decommissioned Case	70
Figure 5.14 Wind Turbine Active Power for the Different Inertia Constants in the Decommissioned Case	71
Figure 5.15 Wind Turbine Active Power for the Different Inertia Constants in the Decommissioned Case	71
Figure 5.16 Comparison of the Frequency Responses for the Base, Fast Inertial Support and Synthetic Inertia Cases	72
Figure 5.17 Comparison of the Active Power Increase in Fast Inertial Support Case and Synthetic Inertia Case	73

LIST OF ABBREVIATIONS

AC	Alternating Current
AGC	Automatic Generation Control
CDF	Cumulative Distribution Function
DC	Direct Current
DFIG	Doubly Fed Induction Generator
FSIG	Fixed Speed Induction Generator
GSC	Grid Side Converter or Controller
HCS	Hill-Climb Search
HV	High Voltage
IGBT	Insulated Gate Bipolar Transistor
LSC	Line Side Converter or Controller
LVRT	Low Voltage Ride-Through
MOSFET	Metal Oxide Semiconductor Field Effect Transistor
MSC	Machine Side Converter or Controller
PDF	Probability Density Function
PI	Proportional-integral
PLL	Phase Lock Loop
PMSG	Permanent Magnet Synchronous Generator
P&O	Perturb&Obserb
PSF	Power Signal Feedback
RES	Renewable Energy System
RoCoF	Rate of Change of Frequency

LIST OF SYMBOLS

C_p	Power Coefficient
f_{grid}	Grid Frequency
H	Inertia Constant
J_{tur}	Turbine Inertia
λ	Pitch or Blade Angle
P_e	Electromechanical Output Power
P_m	Input Mechanical Power
P_{tur}	Turbine Active Power
P_{gen}	Generator Active Power
P_{grid}	Active Power injected to Grid
p_f	Number of Pole
P_{wind}	Aerodynamic Wind Power
S_{base}	Base Apparent Power
ω_m	Generator Speed
ω_{max}	Maximum Generator Speed
T_{Plim}	Torque Limited by Active Power of Wind Turbine
T_{Slim}	Torque Limited by Apparent Power of Wind Turbine

CHAPTER 1

INTRODUCTION

1.1 Global Renewable Energy Status

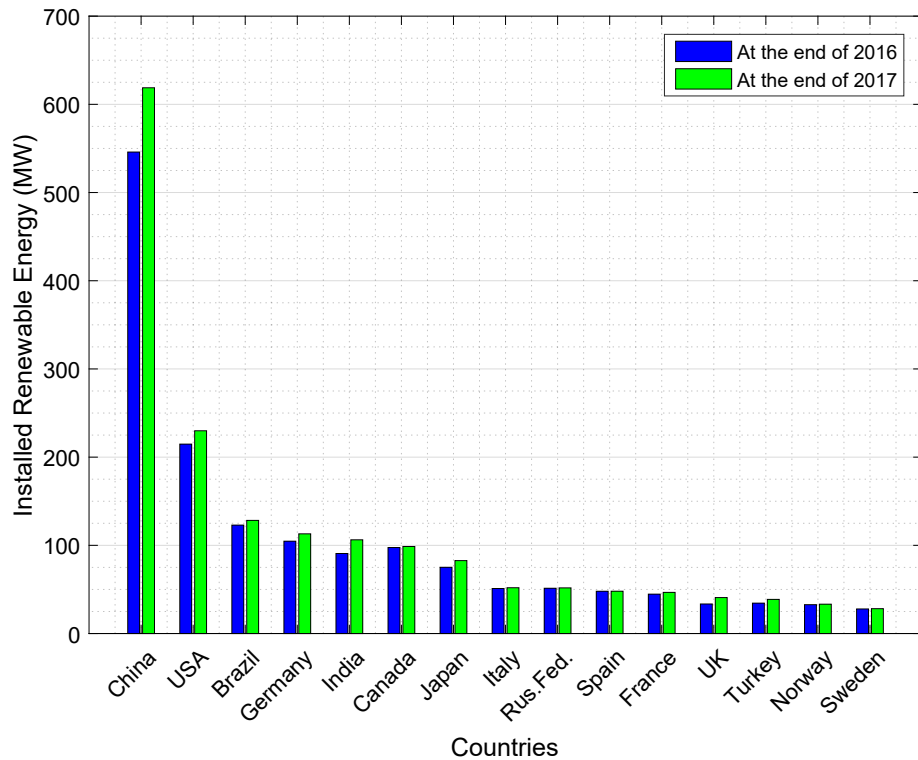


Figure 1.1: Installed Renewable Energy Capacity of Leading Countries

Renewable energy is still one of the hottest topics in the power area. The share of the renewable energy systems has been reached significant levels. At the end of 2017, the renewable power capacity has reached 2179 GW throughout the world including hydro power plants [6]. Fig. 1.1 shows the installed renewable energy capacity

for leading countries at the end of 2016 and 2017 [7], [6]. China, USA, Brazil and Germany constitutes almost half of the world total capacity. China has the biggest installed renewable capacity so far and increased its capacity by 73 GW in 2017 which is very close to the whole installed electrical power of the Turkey. This indicates the severity of the growing renewable demand.

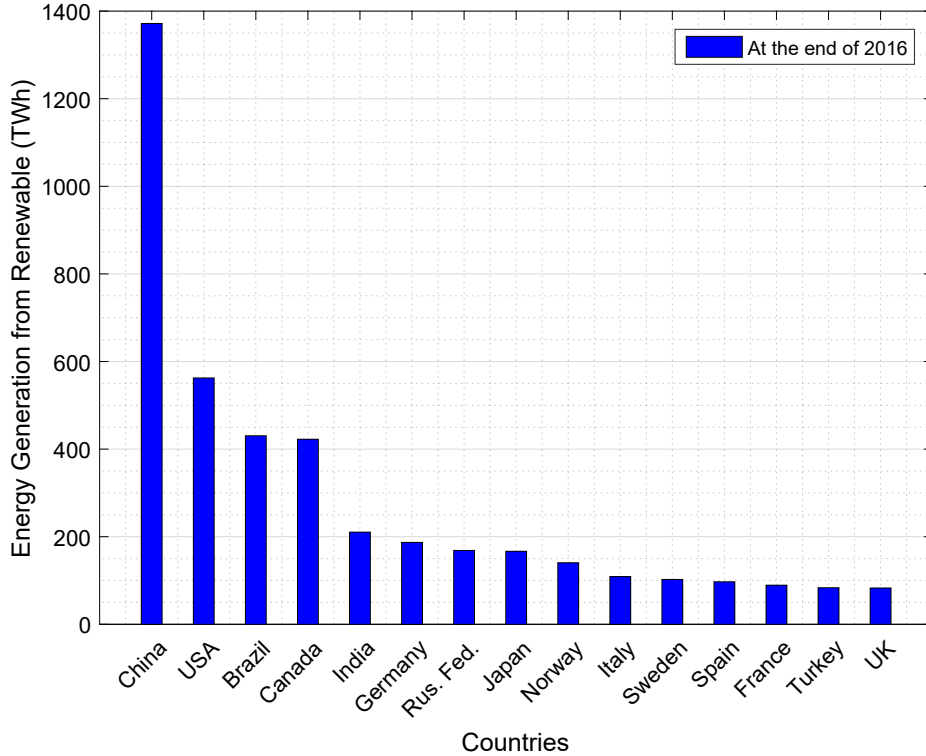


Figure 1.2: Renewable Energy Production of Leading Countries

Fig. 1.2 shows the energy production from renewable energy systems International-RenewableEnergyAgency2017. It is obvious that China, USA and Brazil produces highest amount of energy from renewable since they already have the highest installed capacity. However, India and Canada produces more energy than Germany even though Germany has more installed renewable capacity. This result is due to the fact that renewable energy production is dependent on parameters such as solar radiation and wind speed depending on the renewable source. This can be better observed in Fig. 1.3 which shows the average energy generation from per MW renewable energy sources in 2016 [7]. For a MW renewable energy system, Germany produces the lowest amount of energy meanwhile Canada and Norway produce highest amount

among these countries. Turkey has one of the lowest installed capacity and energy generation from renewable systems among the listed countries. However, it is listed in the middle of these countries due to its high potential for renewable energy systems.

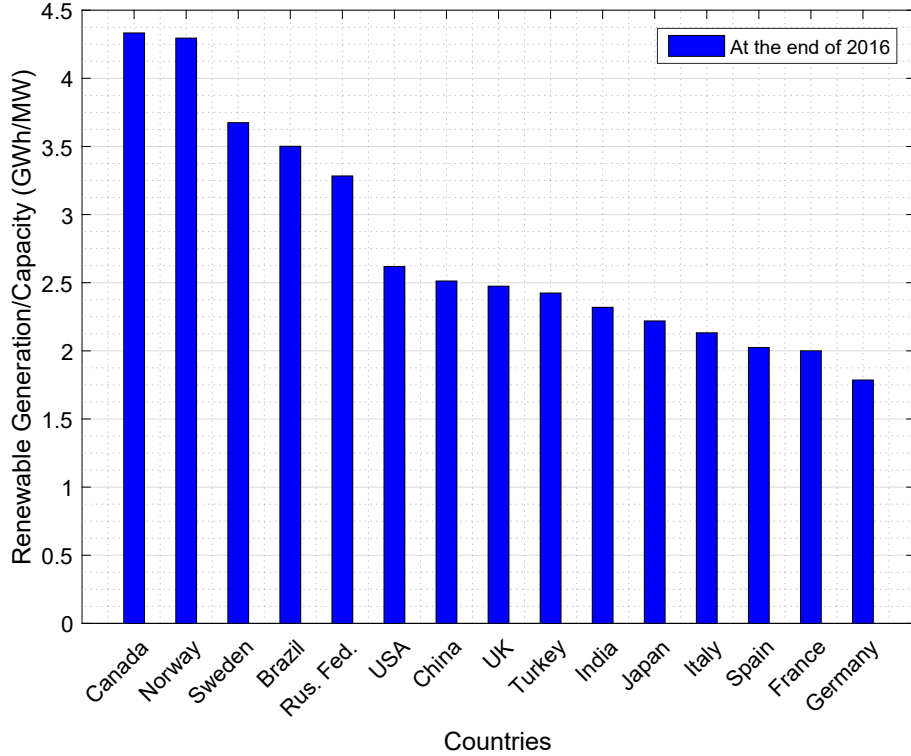


Figure 1.3: Average Renewable Energy Generation per MW in 2016

1.1.1 EU 2020 Goals

In 2008, 20 20 by 2020-Europe's Climate Change Opportunity report has been released by EU Commission and two key targets are set for 2020 [8]:

- At least 20 % reduction in greenhouse gases (GHG) by 2020
- Achieving 20% renewable energy share in energy consumption of EU by 2020

The Renewable Energy Directive is published in 23 April 2009. This directive has set national binding targets for EU countries in order to accomplish the 20% renewable

energy target for EU and 10 % target for the renewable energy usage in the transport. [9] As a result, each EU country has been determined their national action plans. In order to achieve the 20 % target, each member state determine their own targets ranging from 10% in Malta to 49% in Sweden. According to the latest release by Eurostat, renewable share of the EU in energy consumption has reached 17 % in 2016 [1]. Moreover, eleven of EU member states has already achieved their 2020 targets. Renewable shares of EU members are shown in Figure 1.4.

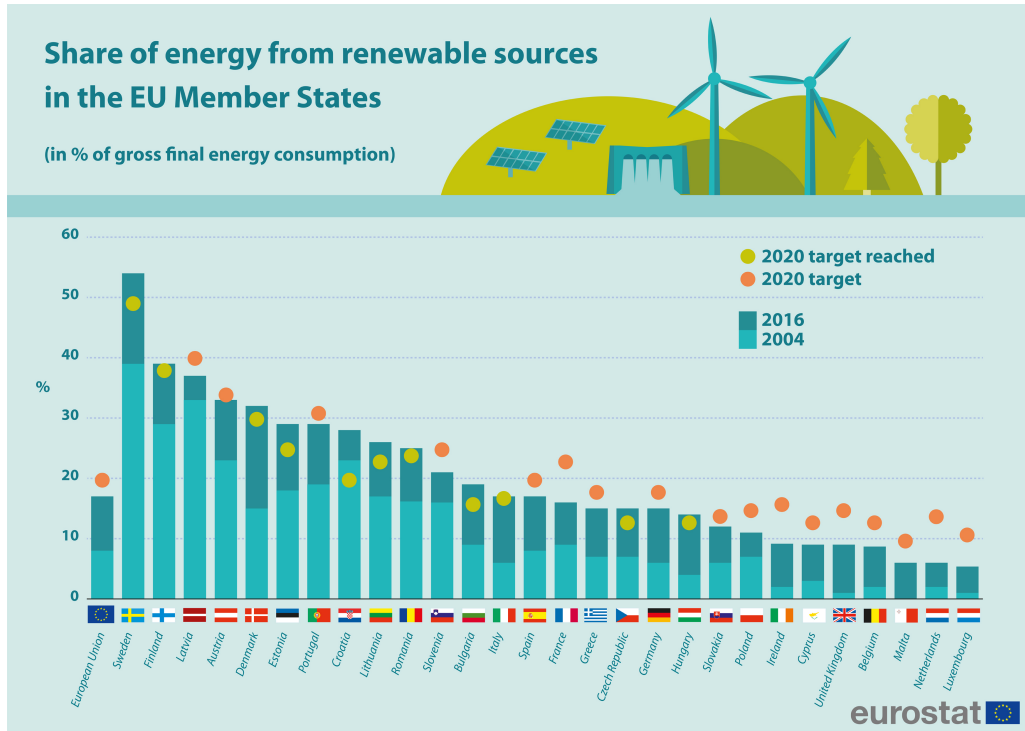


Figure 1.4: Renewable Targets of EU Member States [1]

1.1.2 Wind Energy Status

Wind power has the highest share in the installed renewable energy capacity except for hydro power. The wind power capacity at the end of 2017 has reached 514 GW worldwide [6]. The wind power capacity of the leading countries is shown in the Fig. 1.5. As in the case of total installed renewable energy capacity, China and USA have also the highest installed capacities in the wind power capacity.

The energy production from wind energy is shown in the Fig. 1.6. Even though China

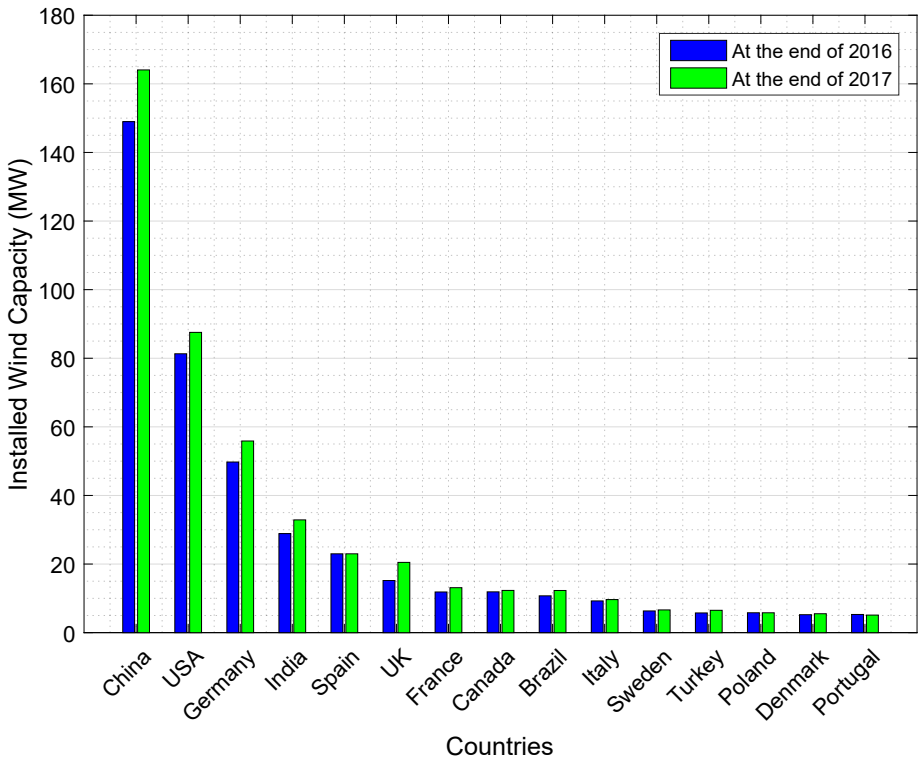


Figure 1.5: Wind Power Capacity of Leading Countries in 2016

has the highest wind power capacity, USA generates highest amount of energy from wind. The energy production per a MW wind energy system is shown in the Fig. 1.7. Denmark, UK and Sweden yield highest energy from per MW wind energy system due to its wind potential meanwhile Germany, India and China generates minimum energy.

1.2 Global Renewable Energy Future

The share of renewable energy is increasing each passing day. Today, reports arguing the possibility of even 100% renewable energy region by region is published [10]. The renewable energy reports estimate the share of renewable energy in the total energy consumption for 2030 and 2050. Figure 1.8 shows the EU renewable energy share for 2030. Moreover, the report published by IRENA (International Renewable Energy Agency) estimates the share of renewable energy in EU as 24% by 2030 which

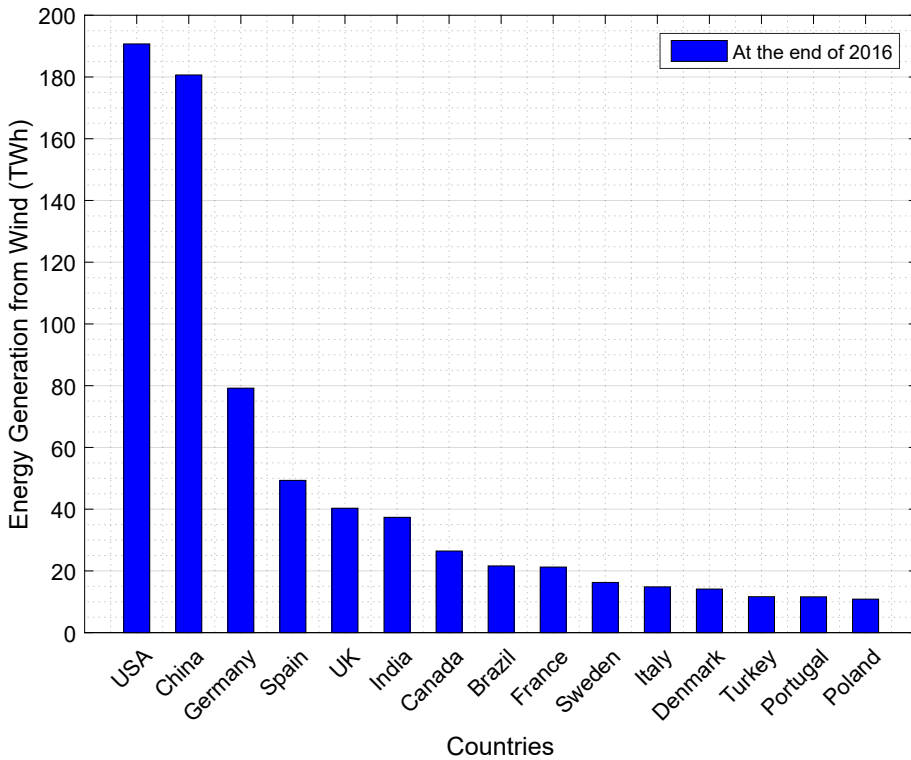


Figure 1.6: Wind Power Production of Leading Countries in 2016

is below proposed target of 27% [3].

Renewable shares of REmap countries in 2010, 2030 reference case and 2030REmap and the world average are also shown in Fig.1.9. The only country whose renewable energy decreases in the 2030 is Nigeria. The reason is that the main source of energy in Nigeria is biogas for the time being. However, the renewable share is expected to decrease dramatically as the industry switches to natural gas.

1.3 Renewable Energy Problems

It is an undeniable fact that renewable energy systems are advantageous in terms of global warming and carbon dioxide emission. Nonetheless, they also have disadvantages to the system operators due to intermittent energy generation profile. First of all, the term intermittent in the literature is related to the variable and uncontrollable nature of the renewable sources [11]. Since the source of the RES is variable, it is not

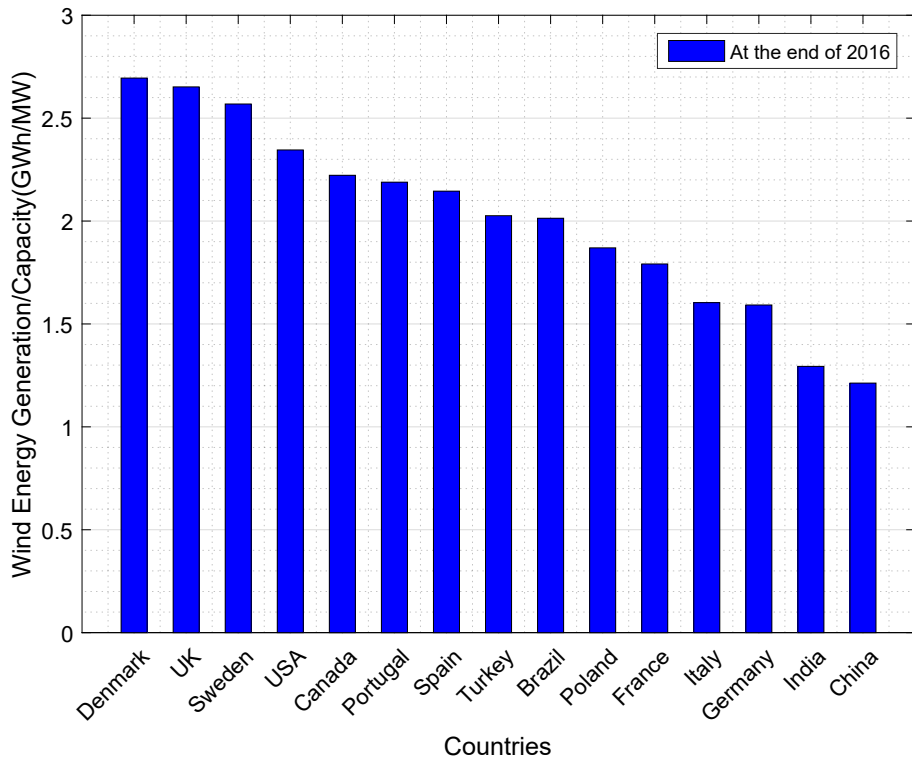


Figure 1.7: Wind Power Production of Leading Countries in 2016

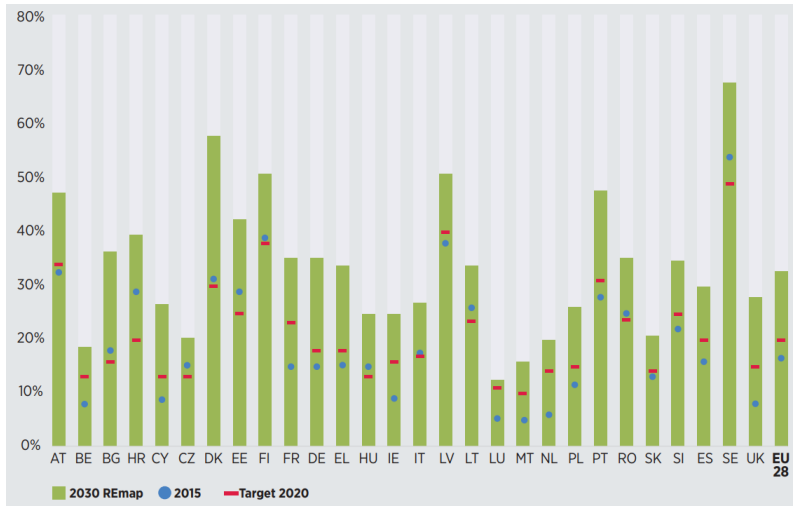


Figure 1.8: Renewable energy share in total energy consumption by EU for 2015, 2020 targets and 2030 potential according to REmap [2]

possible to adjust its output according to the demand. Therefore, the thermal plants have to be in the operation when high wind speeds and solar radiation exist. More-

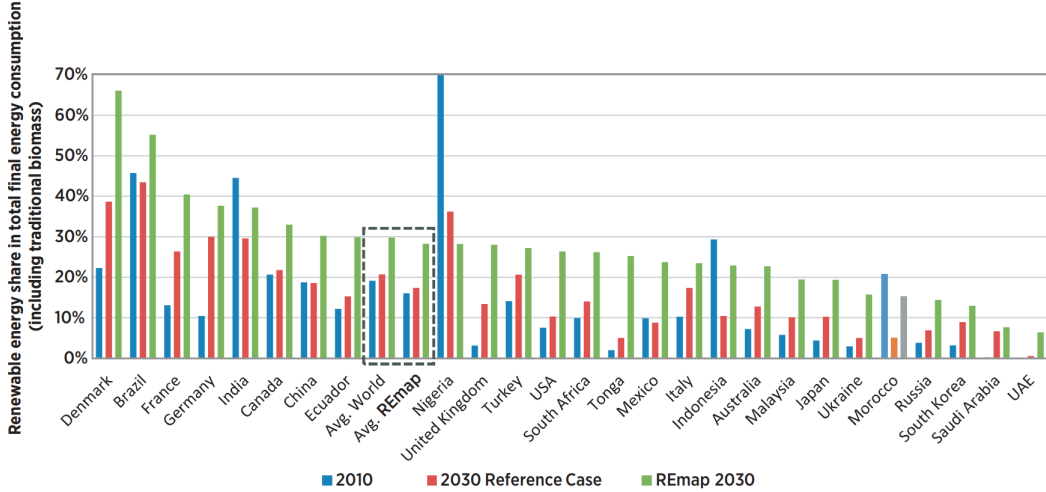


Figure 1.9: Renewable energy shares for 2010, 2030 Reference Case and 2030REmap [3]

over, the system requires additional start-ups and rise from partly loaded plants in order to balance the energy in the system because of the uncertainty of RES. These all create additional costs caused by high share of RES in the system [12]. Moreover, power grid will face with transmission system issues as overloaded transmission lines, changes on the protection and control in the distribution system, greater level of power-factor control and low voltage ride-through (LVRT) requirements when the RES share is increased in the grid [13].

Another challenge of increasing RES is the problem of power system frequency stability. Since the frequency of the power system depends on the balance between generation and consumption, grid operators are responsible for adjusting the generation in order to maintain a constant frequency. However, the renewable energy generation is strictly dependent on the renewable source i.e. solar radiation or wind speed. Therefore, renewable systems makes the system operation harder due to their intermittent and uncertain power generation profiles. Moreover, as the renewable systems with power electronics interface increase in the electricity grid, the grid equivalent inertia decreases. In [14], the reduced grid inertia due to the high DFIG wind turbine penetration is emphasized. Moreover, the results of the reduced grid inertia following a disturbance is listed as:

- increased effective aggregated angular acceleration of synchronous machines

which require high restoring forces

- high rate of change of frequency and hence, decreased frequency nadir

It should be noted that this problem is not specific to DFIG wind turbines but renewable energy systems which are connected to grid with power electronics. Conventional synchronous generators rotates with synchronous speed which is proportional to grid frequency. If the grid frequency decreases, then the synchronous speed also decreases. In this case, the generator active power is increased inherently due to kinetic energy extraction from the generator inertia. The increase in active power provides action time for primary controllers and crucial for frequency stability. Type-1 and Type-2 wind turbines are directly connected to grid. Hence, the frequency deviations affects the active power output of such wind turbines [15]. Nonetheless, active power output of renewable energy systems with power electronics such as Type-3 and 4 wind turbines and photovoltaic systems is not affected from the grid frequency deviations. Therefore, these system have no contribution to the grid inertia whether the system includes inertia or not. Hence, the aggravated grid inertia is reduced with the penetration of RES. The comparison for different type of generators is made in [16] and listed in Table 1.1.

Type of the generator	Inertial Response Behaviour
Conventional Synchronous Generator	++
Fixed Speed Induction Generator (FSIG)	+
Doubly Fed Induction Generator (DFIG)	-
Variable Speed Wind Turbine Generator (Connected with Full Scale Power Electronics)	None

Table 1.1: Comparison of Different Type of Generators for Inertial Response Behaviour

Another reason for the decrease in the grid inertia is the de-commitment or dispatch of the conventional sources due to economic concerns. Since the renewable energy has the lowest cost for energy production, it preferred instead of conventional generators. As a result, conventional generators are dispatched to a lower generation profile or taken-off from operation.

Note that grid inertia is directly related to the amount of load in the system in addition to the share of RES. Therefore, the amount of online generator fluctuates within time. Hence, the scenario in which the system has low demand and also high renewable generation is the most critical one since the lowest grid inertia will be faced in the network.

1.4 Literature Review

Studies regarding inertial support date back to early 2000s. In the study [17], the effect of the increasing wind energy penetration has been investigated. The study concludes that increasing share of wind energy increases the primary reserve requirement for the successful grid operation. The increased frequency deviations, especially in light load conditions (high wind generation with low consumption scenario) can be mitigated in the system as long as the wind generation provides inertia support. Study in [18] states that DFIG wind turbines are de-coupled from power system resulting in no contribution to system inertia. A supplementary loop is proposed for reinstating the machine inertia. Moreover, in [19], performance of the supplementary control loop is evaluated with the comparison of the inertial support of a fixed-speed wind turbine. The proposed control loop has been validated in [20] and compared with the droop control in [21].

It is an undeniable fact that renewable energy systems are the most economical way of producing electrical energy due to absence of any fuel cost. Therefore, they are to be operated in their rated power. However, they have to curtail their power in order to leave a margin for droop control. Droop control by wind energy is also studied in the literature. In [15], the inertial support of different type of wind turbines is compared. It is concluded that the Type-4 wind turbines are able to perform better performance for inertial support due to the power electronics interface. Moreover, combination of inertial support and droop control produces better results in these wind turbines.

Fast inertial response is studied in the literature as Torque-Limit based inertial support or Stepwise Inertial Control in the studies [22], [23]. Nonetheless, the support is achieved by the operation in the limit torque independent from the size of the dis-

turbance and the support is ended at the pre-defined generator speed. Still, limits of the support for varying wind speed is not studied as well as the restoration of the generator speed is not discussed.

The concept of the synthetic inertia has been widely studied in the literature since it is a method for renewable energy systems to emulate synchronous generators. In [24], the method is implemented a VSC-HVDC transmission systems in order to improve frequency stability of a weak grid. Study [25] focuses on the implementation in the PV systems in a coordination with energy storage systems. In the studies [16], [26], the method is implemented on a variable speed wind turbines. However, the capability of the wind turbines are not studied in the literature. Practical limits of the inertial support has been studied in [27] by varying the inertia constant to be emulated. However, the practical limits in terms of maximum achievable power and turbine internal parameters are not focused in the study. Moreover, the studies does not compare the two main method of the inertial support namely, fast frequency support and frequency based method. Finally, the studies does not focus on the wind speed for the inertial support capacity.

1.5 Thesis Motivation

The frequency of the electric grid depends on the balance between generation and consumption. Grid operators are responsible for maintaining this balance so that frequency of the grid is maintained between allowed dead-band. In order to achieve this purpose, power generation is adjusted according to the consumption value. However, the balance between supply and demand might be disturbed with unintentional generator trip or instant load connections. Grid frequency decreases such instants until the generation is increased to arrest the frequency. Inertia of the electric grid provides additional power from the stored kinetic energy and avoid the system frequency from decreasing down very fast. That is called as inertial support and it is very important for power system frequency stability.

Although renewable energy systems are beneficial for environmental concerns and lower energy cost, higher renewable penetration also brings operational challenges

for system operators. One of the most important problem that comes with renewable energy is the power system frequency stability. With the high renewable penetration, grid aggravated inertia decreases. As a result, grid frequency deviates steeper for disturbances. To avoid steeper frequency declines in the grid, all generation technologies should provide inertial support for the frequency disturbances.

Wind energy systems, especially variable speed wind turbines with full scale power electronics are the most promising renewable energy systems that can contribute to grid frequency stability thanks to their high inertia in their blades and generator and also their back-to-back converters that give ability to control its active power. Therefore, wind energy conversion systems are required to participate in ancillary services for frequency stability in order to reach a stable power system network in the upcoming future.

In this study, the limits of the inertial support is investigated in the different wind speeds. By considering the wind speed status, the potential of the wind turbine is revealed for the frequency stability analysis. Moreover, fast frequency response and synthetic inertia support is both implemented on a variable wind speed turbine to investigate their contribution to electricity grid in the frequency disturbances.

1.6 Thesis Outline

This thesis study focuses on the inertial support capability of variable speed the wind turbines. The thesis starts with a brief summary of the renewable energy status in Chapter 1. By reviewing the share of the renewable energy systems and the targets for upcoming future highlight the importance of the frequency stability studies. In the Chapter 2, the frequency concept in power systems is extensively described. Since the conventional power generation units are replaced or preferred over renewable energy sources, the electricity grid is facing with frequency stability issues due to the absence of inertia-less units. Therefore, the behaviour of old-fashion power plants are described under frequency disturbances. Since the existing variable speed wind turbines require modification in order to integrate to electricity grid, detailed modelling of these wind turbines is presented in Chapter 3. The modification in order to mimic

synchronous generator behaviour is also described in this chapter. In this way, wind turbines with full scale power electronics are able to adjust their active output power according to the frequency deviations in the point of interconnection.

The limits of the active power increase is investigated in Chapter 4. The ability of increasing its active power output is already presented in the literature. However, the amount of additional power based on the wind speed is studied. Moreover, the real wind speed measurements are utilized in order to find the probability of such increased power is detected. It is to note that the amount of the inertial support in this chapter is not dependent on the rate of change of frequency. This chapter only explores the capability of the wind turbine for a defined wind speed. Inertial support based on frequency deviations as in the case of conventional synchronous generators are studied in the Chapter 5 on a P.M. Anderson 9 bus test case. Different inertia constants are emulated on a wind farm to see the improvements on the power system frequency stability. Test case is modified with different combinations in which the system is penetrated with wind farm with/without generator decommission are studied in this chapter. The conclusion drawn in this thesis is presented in the Chapter 6.

CHAPTER 2

POWER SYSTEM FREQUENCY STABILITY

2.1 Synchronous Generator and Synchronous Speed

Synchronous machines produce torque only in synchronous speed. This is why they are equipped with damper windings which are basically induction machine windings. If the frequency of grid changes, damper windings create a torque which creates a force to synchronize the speed to the grid frequency. Two type of damper windings are given in Fig. 2.1.

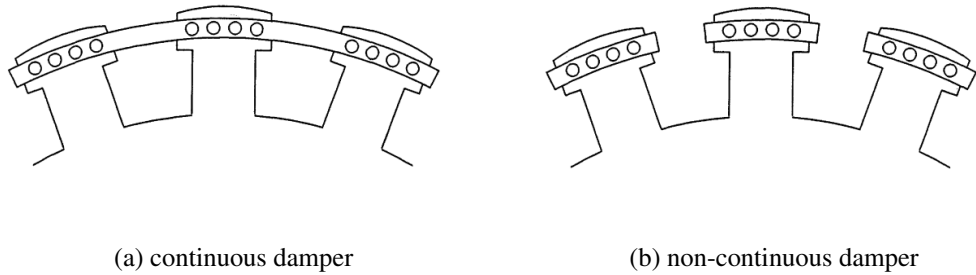


Figure 2.1: Damper windings in a synchronous generator [4]

The synchronous machines keep their operation in the synchronous speed thanks to the damper windings in the rotor. Relation between grid frequency and the synchronous speed is given in Eq. (2.1) in terms of rpm. [4]. This equation can be better observed in Eq (2.3).

$$n_s = \frac{120f}{p_f} \quad (2.1)$$

$$n_s = \frac{60}{2\pi} \omega_{syn} \quad (2.2)$$

$$\omega_{syn} = \frac{4\pi f}{p_f} \quad (2.3)$$

where n_s is the synchronous speed in rpm, f is the grid frequency in Hz, p_f is the number of poles of the generator and ω_{syn} is the synchronous angular speed in rad/s.

2.2 Swing Equation

Speed in synchronous machines changes according to the net torque acting on the rotor. Therefore, the speed is maintained constant unless there is no difference between mechanical and electromechanical torque. The equation of motion is given in Eq. (2.4) where J is aggravated moment of inertia of the generator and the turbine in kgm^2 , T_m and T_e are mechanical and electromechanical torques in Nm .

$$J \frac{d\omega_m}{dt} = T_m - T_e = T_a \quad (2.4)$$

In power system network, the power ratings of the generators and corresponding moment of inertia values varies. Hence, it is more convenient to use inertia constant, H whose unit is seconds and varies between 2 and 9 [4]. Inertia constant is defined as the ratio of kinetic energy stored in the inertia to the power rating of the generator as in Eq. (2.5) where ω_{0m} denotes the rated angular velocity of generator in rad/s and S_{base} is the rated apparent power in VA.

$$H = \frac{\frac{1}{2} J \omega_{0m}^2}{S_{base}} \quad (2.5)$$

Substituting Eq. (2.5) into Eq. (2.4) and replacing units to per-unit quantities yield the relation of frequency with power and inertia constant as in Eq. (2.10).

$$J = \frac{2H}{\omega_{0m}^2} S_{base} \quad (2.6)$$

$$\frac{2H}{\omega_{0m}^2} S_{base} \frac{d\omega_m}{dt} = T_m - T_e \quad (2.7)$$

$$\frac{2H}{\omega_{0m}^2} S_{base} \omega_m \frac{d\omega_m}{dt} = P_m - P_e \quad (2.8)$$

$$2H \frac{\omega_m}{\omega_{0m}} \frac{d(\omega_m/\omega_{0m})}{dt} = \frac{P_m - P_e}{S_{base}} \quad (2.9)$$

$$2H \overline{\omega_m} \frac{d\overline{\omega_m}}{dt} = \overline{P_m} - \overline{P_e} \quad (2.10)$$

2.3 Frequency in Power Systems

The frequency in a power system is related to the speed of the synchronous generators and changes according to the swing equation. The frequency of each generator is not the same in the network since each generator does not have the same speed. There are always fluctuations in the power system. However, the network can be assumed as a single generating unit by neglecting this assumption. The swing equation basically investigates the relation between mechanical and electromechanical powers and the rate of change of angular speed of a generator. Therefore, the speed of a generator remains constant if the mechanical and electromechanical powers are equal.

If the electricity grid is considered as a single generator, the inertia of the equivalent generator is aggregated from each generator in the network. In this case, average frequency in the network can be found as in Eq. (2.11)

$$2H_{sys} \overline{f_{sys}} \frac{d\overline{f_{sys}}}{dt} = \overline{P_m} - \overline{P_e} \quad (2.11)$$

where P_m is the aggregated mechanical input power of the generators meanwhile P_e is the aggregated electromechanical output power. In other words, the system frequency depends on the balance between generation and consumption. Note that generation means the input mechanical power of the generators.

The behaviour of the frequency in electric grid is depicted in Fig. 2.2. As it can be seen from the water level in a container analogy, the frequency of the system is dependent on the in-flow and the out-flow. Therefore, in the electricity grid, frequency increases as the aggregated input power is higher than the aggregated output power. Note that, the direction of the frequency is dictated by this balance. Having a constant

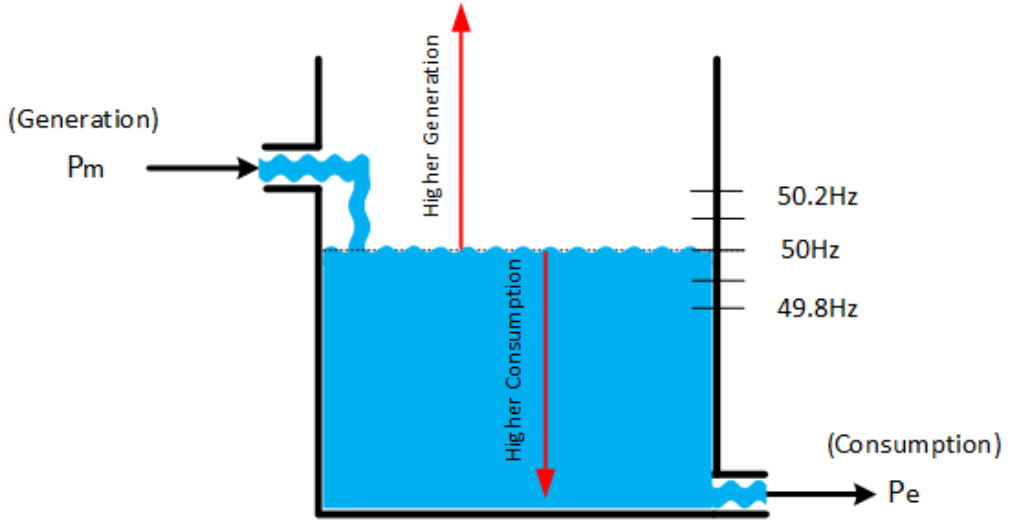


Figure 2.2: Frequency behaviour in electric grid with the water level in a container analogy [5]

49.8Hz frequency does not mean that consumption is higher than generation. If the frequency is constant, then the input mechanical power is equal to output power.

2.3.1 Primary Frequency Control

Having a constant frequency is one of the most important responsibilities of a system operator. In order to have a constant frequency, supply is being adjusted according to the demand continuously. By doing so, the system frequency varies between a band-gap. The variation depends on the disturbances which are generally a sudden generation outage or instant load connection. The size of the disturbance determines the severity of the frequency change and there are three main mechanisms to arrest the frequency changes in the system.

Following generator outage or sudden load connection event, frequency start decreasing. The slope of the frequency is dependent on the severity of the event by means of power and the available inertia of the power system. Such frequency disturbance requires increased input power. However, the increase in the input mechanical power should be activated very fast and should be automated. This responsibility is assigned to generating units with primary control. The active power generation of these units is increased or decreased by the governor depending on the network frequency di-

rection. Note that each generator in the power system does not necessarily perform primary control function. In this case, their active power generation is independent from the network frequency. Hence, the decrease in the frequency is arrested by the primary frequency control. The primary controllers act during a few seconds following a disturbance. They keep their operation up to 30 minutes.

2.3.2 Secondary and Tertiary Control

The frequency is recovered back to nominal value with the Secondary Frequency Control action. This controller might be a single or multiple centres that monitor the frequency and adjust the generation accordingly. They are also called as Automatic Generation Control (AGC) systems and their action takes a few minutes. The final frequency control mechanism is the Tertiary Frequency Control. If the frequency is not recovered back to nominal value with the secondary controllers, tertiary frequency controllers manually activates the load shedding which is an undesired situation by the network operator. However, it is an emergency case which might result in black-out and requires immediate action.

CHAPTER 3

WIND TURBINE MODELLING

3.1 Variable Speed PMSG Wind Turbines

The share of variable speed PMSG wind turbines is increasing worldwide due to the high efficiency and torque density. This type of wind turbines are equipped with full-scale power electronics which enable the turbine to have wide speed range. Even though the price of the permanent magnet fluctuates with time, the reliability and high efficiency of this type of turbine increase its share in the market.

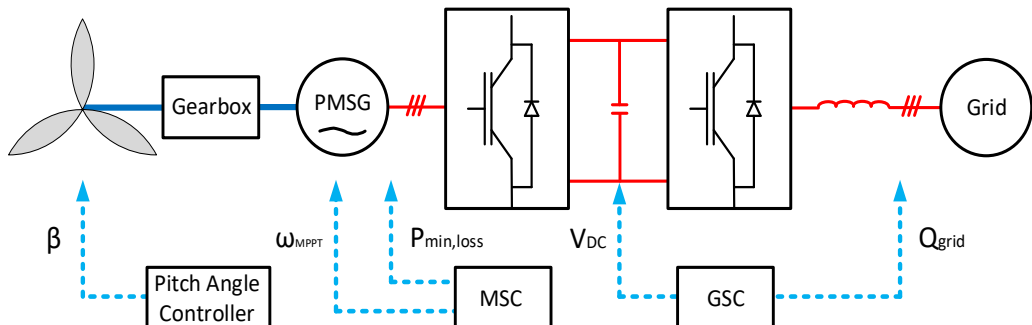


Figure 3.1: Variable Speed Geared Wind Turbine Model

Fig. 3.1 shows the modelling of variable speed PMSG wind turbine. The source of the power in these systems is the wind itself. The power is captured from the wind with the help of three-blade turbine. Three-blade turbine is the aerodynamic part of the system and it applies a aerodynamic torque to gearbox. In fact, this torque is the source of the movement and dictates the direction of the movement. Aerodynamic torque is applied to gearbox which establishes the connection between turbine and generator. In variable speed wind turbines, stator of the PMSG is not directly connected to grid. A back-to-back converter is used between generator and the elec-

trical grid to ensure that the turbine speed is independent from the grid frequency. The converter which is connected to PMSG is called Machine Side Converter (MSC) meanwhile the one connected to grid is called Grid Side Converter(GSC). Moreover, GSC is connected to grid with a filter in order to filter out high frequency currents due to switching action.

3.1.1 Aerodynamic Model

Aerodynamic model is the sub-model that captures power from the wind. The output of this block is the aerodynamic torque that rotates the turbine. However, the wind speed is not the only input. Turbine speed and pitch angle are also the inputs of the system since they affect the mechanical power that is captured from the wind.

The aerodynamic power of wind is given in Eq. (3.1) where ρ_{air} is air density in kg/cm^3 , R is the blade radius in m abd v_{wind} is the wind speed in m/s . Note that this is the available power of the air that is striking the turbine swept area and it is not possible to extract that amount of energy. Otherwise, the air would be standstill behind the wind turbine [28].

$$P_{WIND} = 0.5\rho_{air}\pi R^2 v_{WIND}^3 \quad (3.1)$$

The wind turbine captures a fraction of the available wind power that is denominated as power coefficient C_p . Therefore, turbine power captured from wind can be found with the Eq. (3.2).

$$P_{TUR} = C_p P_{wind} \quad (3.2)$$

Power coefficient determines the amount of power to be captured from wind and it is a non-linear function of the tip speed ratio, λ and pitch angle, β . Tip speed ratio is a parameter proportional with turbine speed. It can be defined as the ratio of the speed in the turbine tip to the wind speed as in the Eq. (3.3). Power coefficient for a specific tip speed ratio and pitch angle can be found with the Eq. (3.4) and (3.5) where c_1 is 0.5176, c_2 is 116, c_3 is 0.4, c_4 is 5, c_5 is 21 and c_6 is 0.0068 [29].

$$\lambda = \frac{\omega_{tur}R}{v_{wind}} \quad (3.3)$$

$$C_p(\lambda, \beta) = c_1(c_2/\lambda_i - c_3\beta - c_4)e^{-c_5/\lambda_i} + c_6\lambda \quad (3.4)$$

$$\frac{1}{\lambda_i} = \frac{1}{\lambda + 0.08\beta} - \frac{0.035}{\beta^3 + 1} \quad (3.5)$$

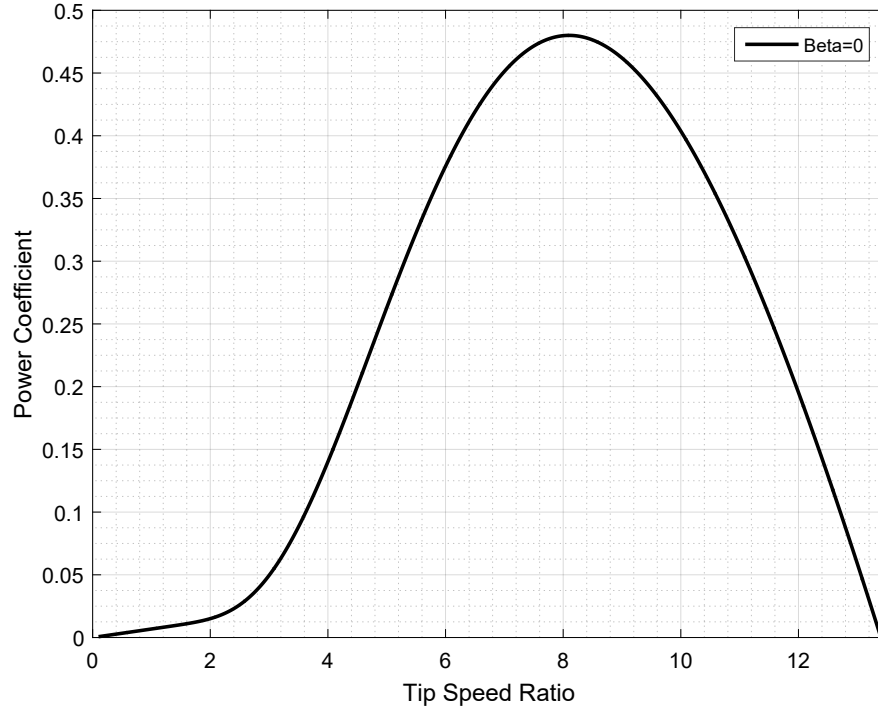


Figure 3.2: Power Coefficient Variation with Tip Speed Ratio under Zero Pitch Angle

Variation of power coefficient C_p is given in Fig. 3.2 for varying tip speed ratio. For the zero pitch angle, power coefficient has the maximum value of 0.48 for the tip speed ratio of 8.1. In order to ensure that the maximum of wind power is extracted, wind turbine should rotate a speed that gives the optimum tip speed ratio. This is ensured by the Maximum Power Point Tracking (MPPT) algorithms.

3.1.1.1 Maximum Power Point Tracking Algorithms

In the literature, numerous different methods are presented in order to operate in the Maximum Power Point. Perturb&Observe (P&O) is the most common MPPT method

in the literature [30], [31]. The methods simply creates a perturbation in the generator speed. The change in the generator speed creates also change in the active power output. If the power is increased with this perturbation, the generator speed is again perturbed in the same direction until a decrease in the active power is observed. This method is the simplest method and does not require any calculation or wind speed measurement. However, the algorithm creates oscillations in the generator speed and active power. This method is also called as Hill-Climb Search (HCS) method in the literature.

Another MPPT algorithm is the wind speed measurement method [32], [33]. If the wind speed is estimated accurately, the optimal generator speed can be calculated. However, wind speed estimation is complicated and increases the cost. One other commonly used MPPT algorithm is the power-signal feedback (PSF) control [33], [30], [34]. This method requires maximum power curve of the wind turbine based on the experimental results. A look-up table is constructed with obtained wind turbine speed and active output power values. However, using generator speed and active power measurements is the main drawback of this algorithm. Finally, there are numerous number of much complex MPPT algorithms based on fuzzy-logic [35] or neural-network [36]. However, these MPPT algorithms are out of scope of this thesis. Therefore, optimal generator speed is provided in this study according to the wind speed.

3.1.1.2 Pitch Angle Control

According to Eq. (3.1), wind power increases with the cube of the wind speed. Hence, wind power increases dramatically for the high wind speeds. In order to decrease power, pitch angle i.e. blade angle is increased. Since the power coefficient, C_p is a function of the pitch angle, β , wind power can be curtailed with increased blade angle. Variation of power coefficient for two different pitch angle is shown in Fig. 3.3. Increasing pitch angle by 1.176° decreases power coefficient by 10%.

As long as wind power is below the rated power, the wind turbine is operated in MPPT speed. This is ensured by obtaining optimal tip speed ratio. This means that for zero pitch angle, MPPT speed is increased linearly with wind speed. Before

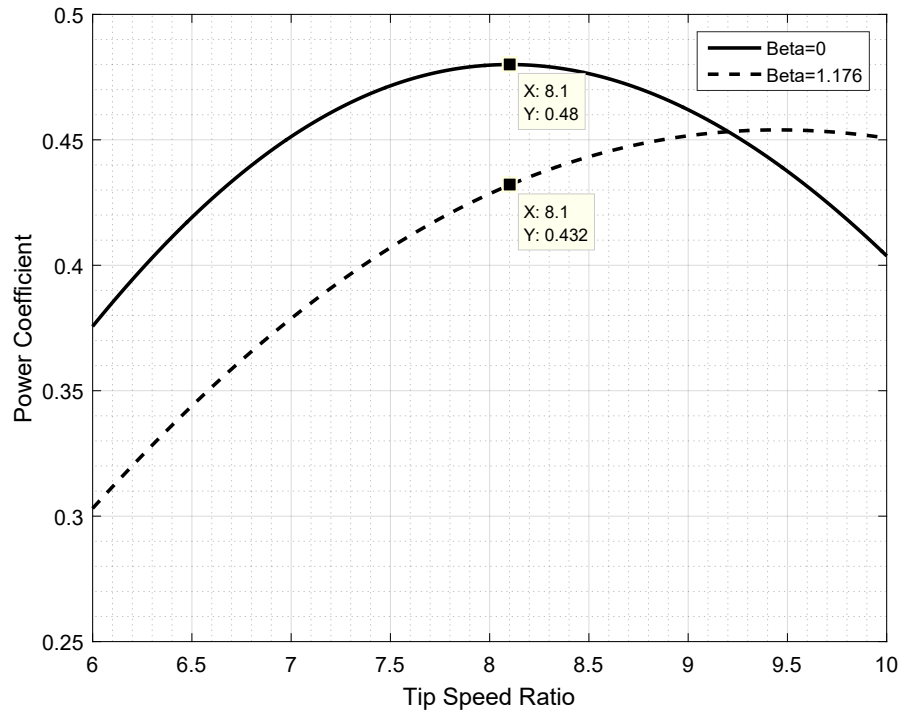


Figure 3.3: Power Coefficient Variation for Two Different Pitch Angle

reaching rated power, MPPT speed might reach maximum generator speed. In this case, wind turbine reference speed will be the maximum generator speed. However, turbine speed cannot be decreased down to reference speed when the torque limit is reached. Hence, the pitch angle should be increased to regulate the turbine speed. Pitch angle controller is depicted in Fig. 3.4. Note that the pitch angle is increased when the speed exceeds maximum generator speed. Otherwise, the pitch angle kept as zero.

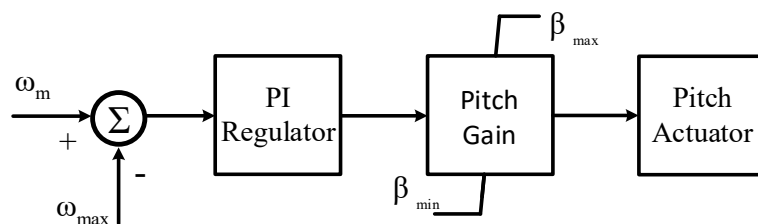


Figure 3.4: Pitch Angle Control Diagram

It is to note that the pitch angle controller takes action as soon as the maximum generator speed is exceeded. Therefore, wind turbine operation deviates from optimal

tip speed ratio. This can also be observed from the variation of power coefficient, C_p with the wind speed for the wind turbine GE 2.75-103 used in this study. Variation of the C_p is shown in Fig. 3.5.

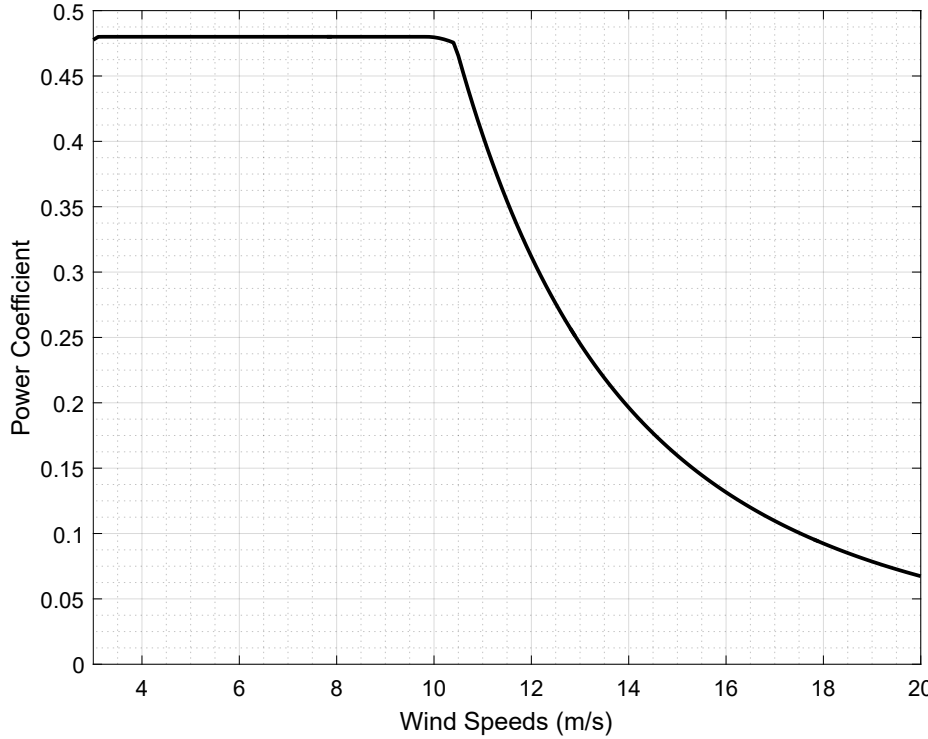


Figure 3.5: Power Coefficient Varion for GE 2.75-103

3.1.2 Gearbox

Variable speed PMSG wind turbines have a gearbox between turbine and generator except for direct-drive wind turbines. The gearbox increases angular speed and decreases the torque in the generator side. By decreasing the rated torque, generator size and cost can be reduced since the generator size is almost proportional to rated torque due to constant shear stress [37]. Moreover, turbine speed is increased to the allowable speed range of the generator which is generally much higher than that of wind turbines. Otherwise, generator should have high pole numbers.

A gearbox model is depicted in Fig. 3.6. They are mainly used for speed and torque

conversion. It should be noted that the gearboxes are not full efficient systems. Therefore, the output torque of the gearbox would be lower than the ratio of input torque to gearbox conversion ratio. Direct-drive systems are based on the elimination of the gearbox systems by direct connection between turbine and generator in order to increase efficiency and reliability [38]. In this study, gearbox system is modelled with 100% efficiency.



Figure 3.6: Gearbox Modelling

3.1.3 Permanent Magnet Synchronous Generator

PMSGs are generally preferred over electrically excited synchronous generators due to high efficiency due to the fact that absence of electrical excitation on the rotor decreases losses. Besides, slip ring is not needed in the generator which also decrease the maintenance. Dynamical equations of the salient pole PMSG are projected on a reference frame which rotates synchronously with magnet flux and given in Eq. (3.6) and (3.7) where R_1 is stator resistance in Ω , L_{sd} and L_{sq} are d and q axis inductances in H , i_{ad} and i_{aq} are d and q axis currents in A , ω is the electrical angular frequency in rad/s ψ_f is magnet flux linkage in Vs [28].

$$v_{1d} = R_1 i_{ad} + L_{sd} \frac{di_{ad}}{dt} - L_{sq} \omega i_{sq} \quad (3.6)$$

$$v_{1q} = R_1 i_{aq} + L_{sq} \frac{di_{aq}}{dt} + L_{sd} \omega i_{sd} + \omega \psi_f \quad (3.7)$$

Another important PMSG parameter is the power in dq frame. The power expression is given in Eq. (3.8). The electromechanical torque can be found by the relation between power and angular speed. The torque expression is also given in Eq. (3.9)

where p is the number of pole pair.

$$P_{elm} = \frac{3}{2}\omega i_{aq}(\psi_f + i_{ad}(L_{sq} - L_{sd})) \quad (3.8)$$

$$T_e = \frac{P_{elm}}{w_m} = \frac{P_{elm}}{w/p} = \frac{3}{2}pi_{aq}(\psi_f + i_{ad}(L_{sq} - L_{sd})) \quad (3.9)$$

Given equations are defined for salient pole machines. If the cylindrical rotor machine is used, the torque equation reduces to the Equation 3.10.

$$T_e = \frac{3}{2}pi_{aq}\psi_f \quad (3.10)$$

3.1.4 Machine Side Converter

Variable speed wind turbines are equipped with the Back-to-Back converters in order to decouple grid frequency and the turbine speed. This gives wind turbine degree of freedom for the rotational speed. In this way, turbine is able to capture the maximum available power from wind. Machine Side Converter (MSC) i.e. Generator Side Converter is the converter that is connected between generator and DC-bus. The three phase generator output AC voltage is converted to DC voltage. Conversion from AC to DC can be achieved by three-arm full bridge converters. This converter can be equipped with uncontrolled, semi-controlled and fully-controlled switches. Fully-controlled switches such as MOSFET, IGBT are commonly used in the industry and gives two control parameters to the user.

Voltages and currents are generally transformed into synchronously rotating reference frame or also called dq frame. Since the frame is rotating in synchronous speed, three-phase phasors are transformed to DC quantities. Therefore, its control becomes easier [39]. Proportional-integral (PI) controllers are associated with the dq control structure due to their satisfactory behaviour interaction to DC variables [40]. Hence, the control in the back-to-back converter is achieved with PI controllers in the dq frame.

The control diagram of the MSC is depicted in Fig. 3.7 according to the study in [41]. In dq frame, it is possible to control two parameters. One of these parameters is the d-axis current. It can be set zero in order to decrease the stator copper losses. The

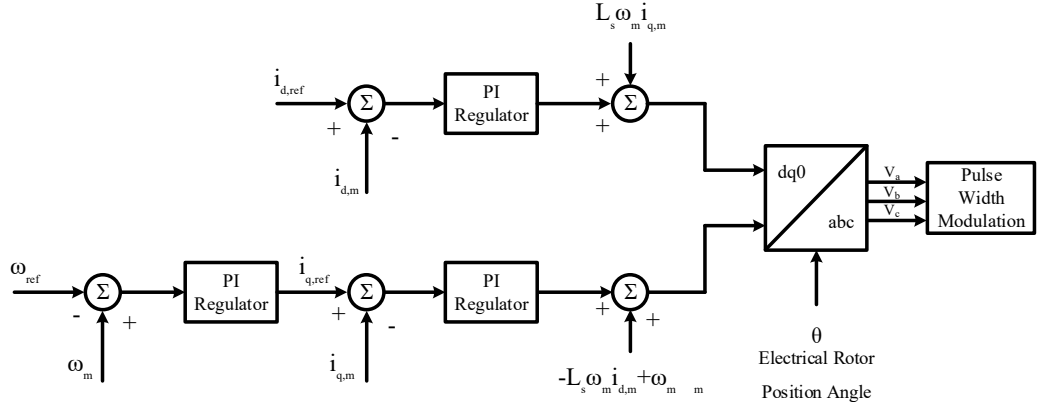


Figure 3.7: Machine Side Control Diagram

other parameter is the q-axis current that is proportional to the electromagnetic torque as it can be observed in the Eq. (3.10). However, q-axis current or torque is controlled in order to regulate the turbine speed. Therefore, turbine speed is adjusted such that the turbine will capture maximum available power in the wind.

3.1.5 Grid Side Converter

Grid Side Converter (GSC) or Line Side Converter (LSC) is the converter that is connected between DC-link capacitance and grid. GSC works as an inverter that injects current synchronous with grid voltage. Currents and voltages are transformed into synchronously rotating frame that is aligned with the grid voltage. Therefore, d-axis current determines the amount of current which is in phase with the grid voltage meanwhile q-axis current determines amount of current that is out of phase with the grid voltage. In other words, injecting d-axis current injects active power to grid meantime q-axis current injects reactive power to grid.

The responsibility of the GSC is regulating DC voltage and the reactive power injected to grid. The control diagram of the GSC is given in Fig. 3.8. As seen from the figure, DC-bus voltage is regulated by controlling the d axis current. If the DC-bus voltage increases above the reference value, d-axis current reference is increased. As a result, active power increases. Increased active power also decreases the DC-bus voltage level. Reference value of the q-axis current is set to zero in normal operation, consequently unity power factor. For Low Voltage Ride-Through studies, q-axis

current is determined according to the reactive power value requirement. [42]

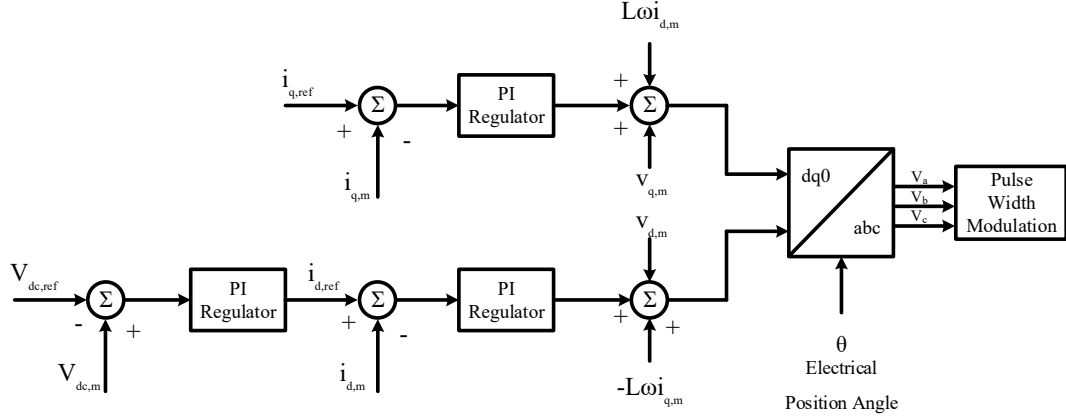


Figure 3.8: Grid Side Control Diagram

GSC is connected to grid through an filter. Therefore, the output voltage of the converter is not equal to the that of grid. The relation between converter voltage, grid voltage and current is derived through Eq. (3.11) to (3.17) where v_c is the converter voltage, v_g is the grid voltage and i_g is the grid current measured in the grid side. As it is observed in Eq (3.16) and (3.17), converter side voltage includes same axis grid voltage and a term proportional to cross axis current which is called cross-coupled term. Therefore, the outputs of the inner PI regulators are compensated and forwarded to Pulse Width Modulation after transformation to three-phase voltages.

$$\bar{v}_c = v_{dc} + jv_{qc} \quad (3.11)$$

$$\bar{v}_g = v_{dg} + jv_{qg} \quad (3.12)$$

$$\bar{i}_g = i_{dg} + ji_{qg} \quad (3.13)$$

$$\bar{v}_c = \bar{v}_g + \bar{i}_g j\omega L \quad (3.14)$$

$$v_{dc} + jv_{qc} = v_{dg} + jv_{qg} + j\omega L(i_{dg} + ji_{qg}) \quad (3.15)$$

$$v_{dc} = v_{dg} - \omega L i_{qg} \quad (3.16)$$

$$v_{qc} = v_{qg} + \omega L i_{dg} \quad (3.17)$$

The PI regulators of the wind turbine model is tuned with trial error method. In this study, the modelled wind turbine is connected to grid with an L filter even though the actual turbine is connected to grid with an LCL filter. However, the actual system would operate better than the modelled case since the the LCL filter has superior performance than L filters [43]. Nonetheless, L filter has provided sufficient performance for the successful operation of the wind turbine in this study regardless from the power quality standards in the output current. The active power of the wind turbine under varying wind speed is given in the Fig. 3.9.

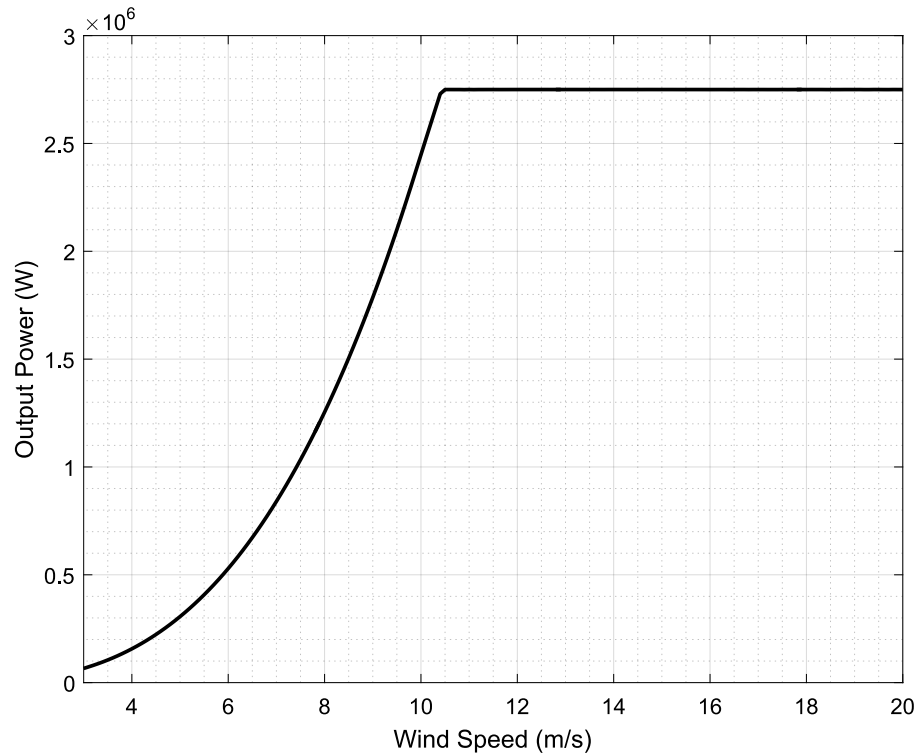


Figure 3.9: Variation of the Active Power of the Wind Turbine

3.2 Synthetic Inertia Implementation

As explained in Chapter 2 Section 2.2, synchronous generators changes its speed according to the balance between input mechanical and electromechanical powers. The inverse case is also true. In other words, if the frequency changes, the electromechanical power of the generators also change. Synthetic inertia is the method that implements this behaviour on the renewable energy systems. It is possible to change the active power output of the wind turbines if these are connected to grid with full scale power electronics. The increase in the active power should be proportional to change of frequency and the inertia of the renewable energy system. Even though renewable energy system does not have inertia, inertial support with desired inertia constant can be implemented in the system as long as a stored energy exists in the system.

In order to implement synthetic inertia in the system, a relation between frequency and active power of the wind turbine should be constructed. Wind turbine in this study is variable speed wind turbine with full scale power electronics. The speed of the turbine is controlled by MSC such that active power is adjusted. Inertial support modification is depicted in Fig. 3.10. The new value of the active power is determined according to the swing equation. However, the wind turbine in this study is operated with a reference speed rather than a reference power. Therefore, the assigned power value should be used in order to yield the q-axis current reference value. Reference q-axis current is derived between the Eq. (3.18) to Eq. (3.21).

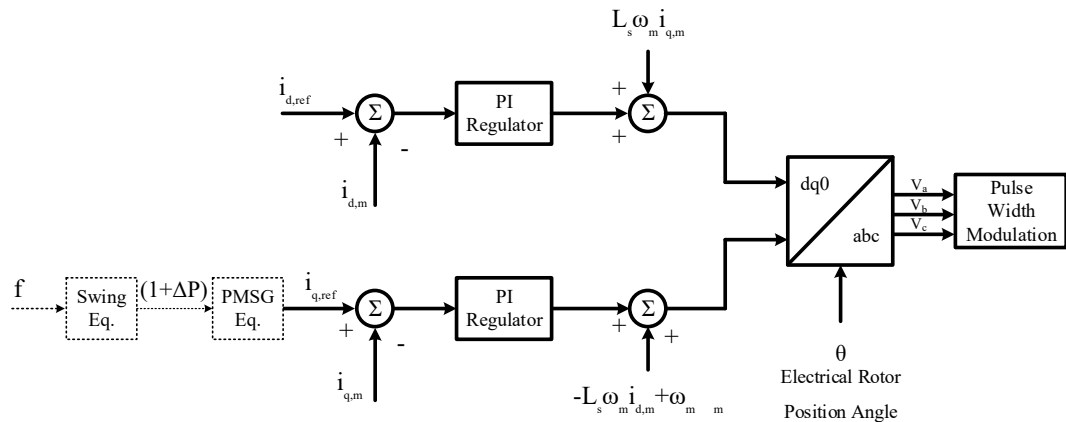


Figure 3.10: Modified MSC for Inertial Support

$$P_{new} = (1 + \Delta P)P_{pre} \quad (3.18)$$

$$T_{new}\omega_m = (1 + \Delta P)T_{pre}\omega_{pre} \quad (3.19)$$

$$\frac{3}{2}p\psi_f i_{q,new}\omega_m = (1 + \Delta P)\frac{3}{2}p\psi_f i_{q,pre}\omega_{pre} \quad (3.20)$$

$$i_{q,ref} = i_{q,new} = (1 + \Delta P)\frac{i_{q,pre}\omega_{pre}}{\omega_m} \quad (3.21)$$

3.2.1 Synthetic Inertia Activation Schemes

Another issue about inertial support is the time instant to trigger synthetic inertia. In the literature, continuous operation, under-frequency trigger and maximum-frequency gradient are discussed [44]. It is obvious that continuous operation would create oscillations in active power output due to the continuous deviations in grid frequency. This is an unrealistic operation and is used for comparison purposes.

Second activation method is the under-frequency trigger which is the activation when the frequency decreases below a threshold value. It can be used for capturing the time instant for the inertial support. However, power grid might be in a stable point even if the frequency is 49.8Hz. Therefore, this method would be unsuccessful depending on the disturbance event.

Third activation scheme is the maximum-frequency gradient trigger. It uses a controller that is very similar to RoCoF relays and tracks the frequency gradient. Once the frequency gradient is below a threshold value, the synthetic inertia is activated. Since the severity of frequency disturbance event is related to the RoCoF, this activation scheme is the most remarkable scheme [44]. In this study, maximum-frequency gradient is used with a threshold value of 0.1Hz/s.

3.2.2 Source of the Inertial Support

Renewable energy systems convert the energy captured from wind or sun to the electrical energy. Hence, the renewable energy systems cannot determine the amount of power in contrast the conventional systems. A thermal power plant, for instance, adjusts its power output as desired. However, the source of power in renewable energy is constant for a definite wind speed or solar radiation. This is why a spare energy is required in order to change the power output.

Energy stored in DC bus capacitance is the only stored energy in PV systems. The amount of energy is given in Eq. (3.22) and negligible for inertial support studies. In the wind energy systems, there exists huge amount of kinetic energy in wind turbine generator and blades in addition to electrostatic energy. The kinetic energy expression is given in Eq. (3.23). Note that J_{total} is the equivalent inertia in the generator side and ω_m is the speed of the generator.

$$E_{electrostatic} = \frac{1}{2} C_{DC} V_{DC}^2 \quad (3.22)$$

$$E_{kinetic} = \frac{1}{2} J_{total} \omega_m^2 \quad (3.23)$$

Note that the amount of kinetic energy is dependent on the generator speed. Therefore, the stored energy in wind turbines changes according to the generator speed. Moreover, it can also be concluded that the energy is dependent on the wind speed. However, the generator speed is kept constant if the wind speed increases above the rated wind speed.

To illustrate the situation better, the electrostatic energy stored in DC bus and kinetic energy in turbine equivalent inertia are compared for GE2.75-103 wind turbine. The wind turbine has a DC bus capacitance of $27mF$ and $1200V$ DC link voltage. The corresponding electrostatic energy is calculated in Eq. (3.24). The generator speed of the corresponding generator is between $550rpm$ and $1735rpm$. The total turbine inertia is $1058.2kgm^2$ in generator side. The minimum and maximum kinetic energy values are calculated in Eq. (3.25) and (3.26). These values are found out to be 90 and 900 times of the electrostatic energy stored in DC bus capacitance.

$$E_{DC-Link} = \frac{1}{2} 27(10^{-3}) 1200^2 = 19.44kJ \quad (3.24)$$

$$E_{kinetic,min} = \frac{1}{2}(1058.2)57.6^2 = 1755.17kJ \quad (3.25)$$

$$E_{kinetic,max} = \frac{1}{2}(1058.2)181.7^2 = 17466.02kJ \quad (3.26)$$

CHAPTER 4

INVESTIGATION OF INERTIAL SUPPORT PRACTICAL LIMITS

4.1 Inertial Support Limits

The source of the power in a wind turbine is the aerodynamic wind power, P_{wind} which is constant for a constant wind speed, pitch angle and generator speed. In the steady state, this power is transferred through MSC as P_{gen} . If there is a difference between P_{wind} and P_{gen} , the difference is either stored in or extracted from the turbine and generator inertia as in the form of kinetic energy. Grid power, P_{grid} is received from MSC and injected grid. The difference between P_{gen} and P_{grid} is stored in or extracted from DC-bus capacitance. The active power flow diagram is depicted in Fig. 4.1.

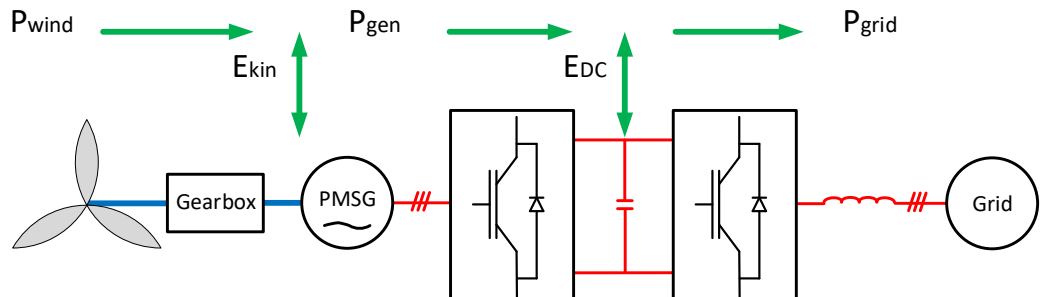


Figure 4.1: Active Power Flow Diagram

As mentioned in Chapter 3, stored energy exists in turbine and generator inertia and DC-bus capacitance. However, it is also stated that the E_{kin} is much larger than E_{DC} even in the lowest generator speed. Therefore, the source of additional power in the inertial support studies is the kinetic energy stored in the equivalent turbine inertia. Besides, the DC-bus voltage cannot be decreased below a threshold value that

is dependent on the grid phase-to-neutral voltage.

Wind turbine active power can be increased by increasing the generator power P_{gen} as long as that power is successfully injected to grid. This can be achieved by adjusting the generator torque since the active power is proportional to electromagnetic torque. However, the active power is also dependent on the generator rotational speed as in Eq. (4.1). The active power can be increased by increasing the turbine torque but the increase is limited by the generator speed. Therefore, the active power increase is also dependent on the wind speed which determines MPPT speed in the steady state.

$$P_{gen} = T_e \omega_m \quad (4.1)$$

It is to note that the source of the additional power is the kinetic energy stored in the turbine equivalent inertia. Therefore, as soon as the power is increased, the turbine and generator speeds start decreasing. Therefore, the electromagnetic torque should be increased steadily to keep the generator power constant. The time duration that generator power is increased and the initial generator speed will determine the final generator speed as in the Eq. (4.2).

$$\int_{t_i}^{t_f} P_{wind} - \int_{t_i}^{t_f} P_{gen} = \Delta E_{kin} = \frac{1}{2} J_{tur} (\omega_f^2 - \omega_i^2) \quad (4.2)$$

As seen from the Eq. (4.1), the generator power is the multiplication of generator torque and speed. In the high speeds, the generator speed ω_m , cannot be controlled with only the generator torque but also with the pitch angle. In this way, the rated power is not exceeded as in the Eq. (4.3) by keeping turbine at the maximum generator speed and the maximum generator torque. However, general practice is employing higher power rating converter than generator active power rating in the variable speed wind turbines [15]. Therefore, higher limit torque, T_{S-lim} can be used in such wind turbine applications by considering the apparent power of the back-to-back converters. Therefore, the maximum power for a wind speed can be defined as in Eq. (4.4).

$$P_{rated} = T_{P-lim} \omega_{max} \quad (4.3)$$

$$P_{max} = T_{S-lim} \omega_{max} \quad (4.4)$$

It is obvious that the maximum available active power is dependent on the generator speed, hence, the wind speed for the corresponding operation time. This is why the

amount of the active power increase also depends on the wind speed. By considering the MPPT speed operation in GE 2.75-103 model variable speed wind turbine, the maximum increase in the active power is shown in Fig. 4.2. The wind turbine can increase its active power by the lowest amount when the wind speed is high. Since the turbine output power is already close to converter maximum power rating, the increase in the active power is much lower than that of low wind speed operations. It is observed that the wind turbine output power can be increased by 0.45 pu when the wind speed is between 5m/s and 8m/s.

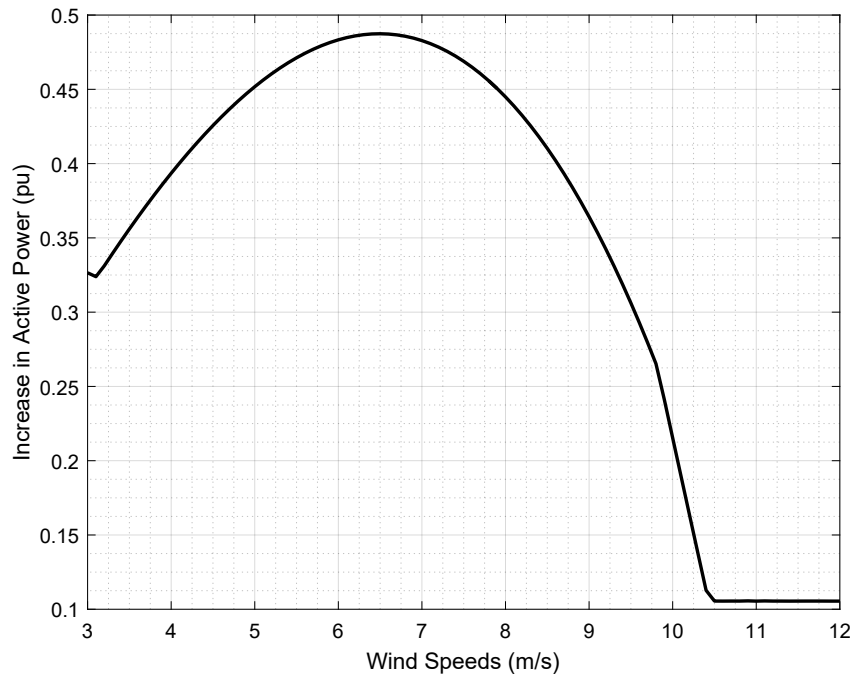


Figure 4.2: Increase in the Active Power Output for Varying Wind Speeds

It is already stated that power system frequency is a function of input mechanical power of conventional synchronous generators and the output active powers. Therefore, frequency disturbances occur due to the imbalance between these. Since the aim of providing inertial support in the form of fast increased active power is to arrest the frequency decline, the increase in the output power is much more important than the total active output power.

4.2 Fast Inertial Support Under Different Wind Speeds

Active power of the wind turbines is determined by parameters such as wind speed, pitch angle and turbine speed. Therefore, combination of these parameters have importance for a possible fast inertial support. In other words, wind turbine under high wind scenario has different potential than that under low wind scenario. Likewise, the resultant states of wind turbines for inertial support would be much different. In this section, the effect of wind speeds will be investigated for fast inertial support. Active power of wind turbines will be increased by different percentages in the fastest way independent of the grid frequency. Turbine internal parameters such as the change in generator speed, turbine and generator torques, DC-link voltage and pitch angle, if any, will be observed. Wind turbine used in this study is GE 2.75-103 model, variable speed PMSG.

4.2.1 Low Wind Scenario

The minimum speed of the wind turbine in this scenario is 550 rpm in the high speed side. Wind speed that will capture the maximum power from wind in this generator speed is found out to be 3.12m/s. In this scenario, the kinetic energy stored in the turbine inertia is minimum and calculated in Chapter 4 in Eq. (3.25). This scenario investigates the case where the least amount of kinetic energy exists in the turbine equivalent inertia. By the fast inertial support provision, the wind turbine speed decreases below the minimum generator speed. However, the resultant minimum generator speed is dependent on the increase in the active power and also the support interval.

4.2.1.1 Fast Inertial Support Limit in Low Wind Scenario

The electricity grid in the upcoming future might require sudden active power release from wind farms for short time durations to arrest steepest frequency declines. Therefore, it is important to observe the maximum achievable power for inertial support studies. The equation Eq. (4.4) implies that wind turbine in the low wind speed

scenario cannot reach rated active power since the generator speed is much lower than the maximum generator speed. However, the electromagnetic torque in steady state is much lower than the limit torque, T_{S-lim} . Therefore, the wind turbine in low speed scenario has the potential for increasing its active power to a significant value. Fig. 4.3 shows the increase of active power to maximum value. The increase is obtained by ensuring the limit torque, T_{S-lim} . However, since the generator speed is decreasing, the active power is also decreasing due to the fact that further increase in the generator torque is not possible.

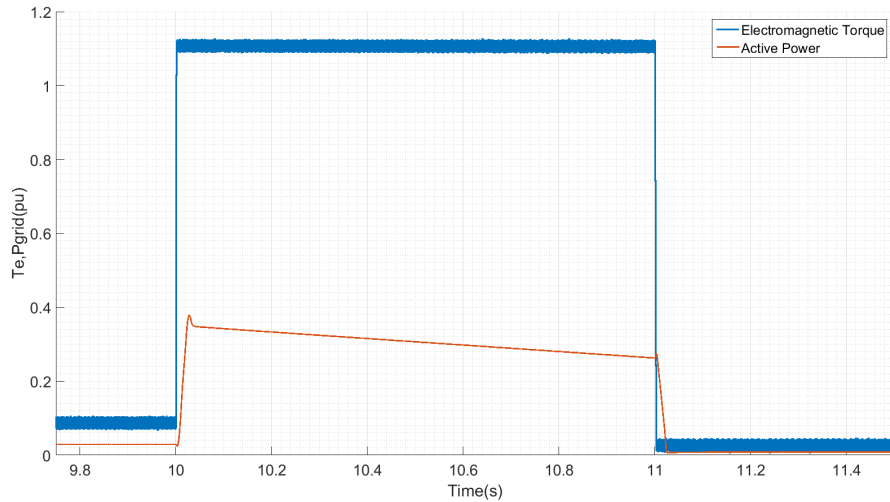


Figure 4.3: Fast Inertial Support Active Power Limit for Low Wind Scenario

Since the turbine is forced to increase its power by high amount compared to pre-disturbance value, the support interval is kept as 1 second. Even in this short duration, the generator speed declines significantly. Variation of the turbine power, P_{tur} and generator power, P_{gen} as well as the generator speed, ω_m is shown in Fig. 4.4. It is to note that turbine might stall if the support duration is extended.

Another important criteria for turbine internal dynamics is the variation of the DC-bus voltage. The DC-bus voltage regulation ensures the complete transfer of the generator power to grid. Therefore, it is critical to have a regulated DC-bus in the inertial support studies. The variation of the DC-bus voltage is shown in Fig. 4.5. The sudden increase in the generator power rises the voltage up to 1.05pu and the voltage is regulated in 150ms. However, the voltage is regulated as soon as the grid power

is increased. DC-bus regulation is directly related to GSC modelling. However, the GSC modelling in this study might be more ideal than the actual case. In reality, DC-bus voltage is highly sensitive to rotor aerodynamic harmonics due to tower shadow and wind shear effects [45]. Therefore, the effect of the fast inertial support on the DC-bus voltage regulation can be better observed with actual parameters of the GSC and the inclusion of tower shadow, wind shear effects. However, they are out of the scope of this thesis study.

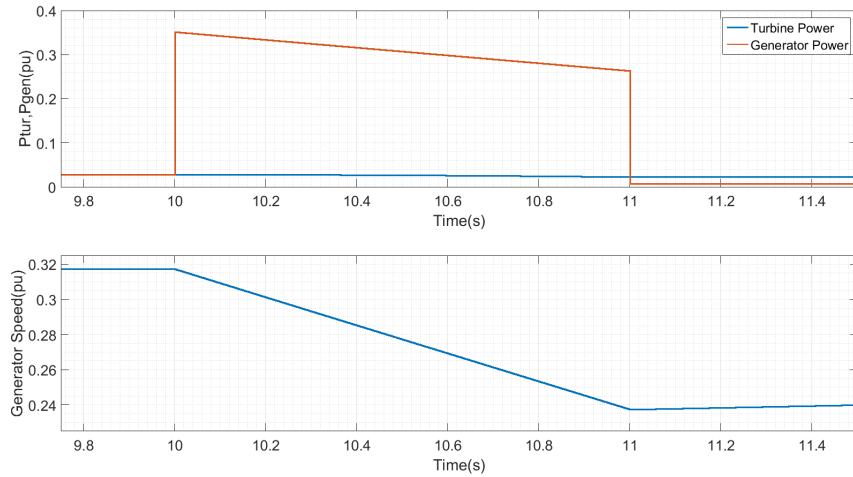


Figure 4.4: Generator and Turbine Power and Generator Speed for Low Wind Speed Limit Case

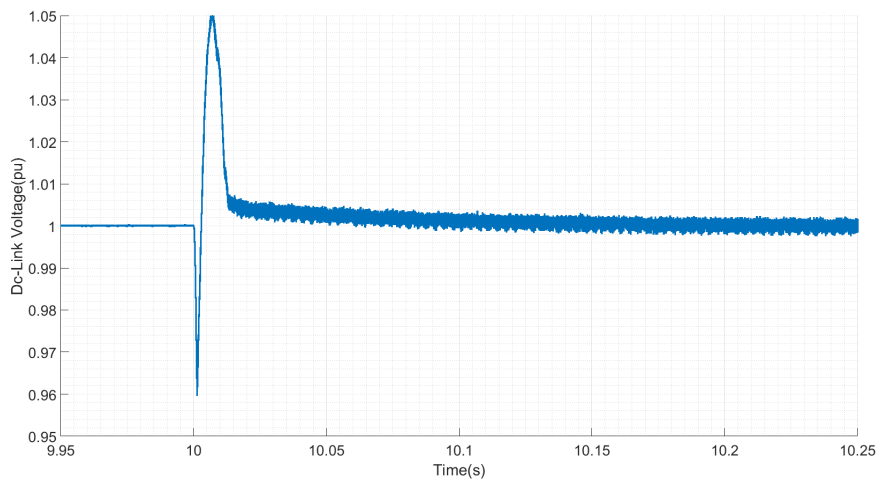


Figure 4.5: Variation of DC-bus Voltage for Low Wind Speed Limit Case

4.2.1.2 Moderate Fast Inertial Support for in Low Wind Scenario

Wind turbines are able to increase its power to significant values even in the low wind speed scenario. However, the time interval is kept as short as possible in order to avoid excessive energy extraction from renewable sources. Nonetheless, the longer support periods can be achievable if the increase in the active power is decreased. Therefore, in this part, the active power of the wind turbine is increased 10% for three different time intervals as 5, 10 and 20 seconds. The active power output of the wind turbine is given in Fig. 4.6. It is observed that turbine power decreases below the nominal value after the support period in order to recover the generator speed. Another observation is the fact that higher support time creates higher dip in the active power in the speed recovery period.

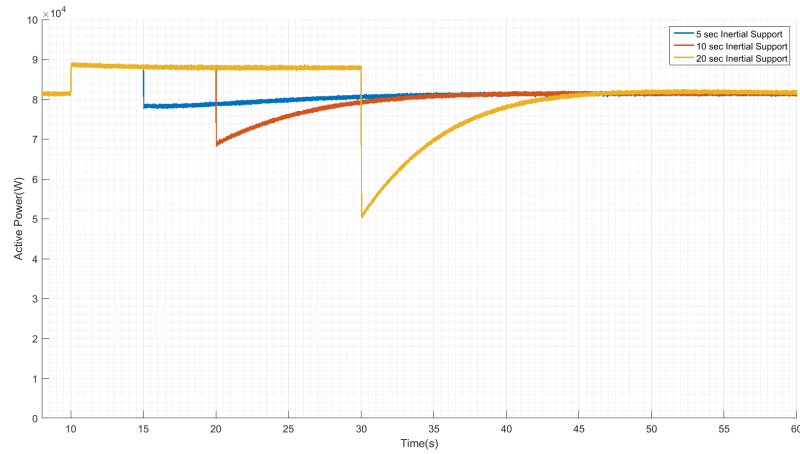


Figure 4.6: Active Power Output of the Wind Turbine for Low Wind Scenario

Generator speed decreases continuously until the support is ended. The generator speeds are shown in Fig. 4.7 for three support times. The decrease in the generator speed is obtained with an increase in the generator torque. The turbine torque, generator torque and generator speed for 5 seconds support is given in Fig. 4.8. The generator torque is increased at $t=10s$ for a time duration of 5 seconds. Turbine torque increases slightly with decreasing speed. However, the increase in the turbine torque is negligible when it is compared to the increase in generator torque as shown in zoomed graph. Therefore, the turbine torque can be considered to be constant for the support period meanwhile the generator torque is increased. Turbine and generator

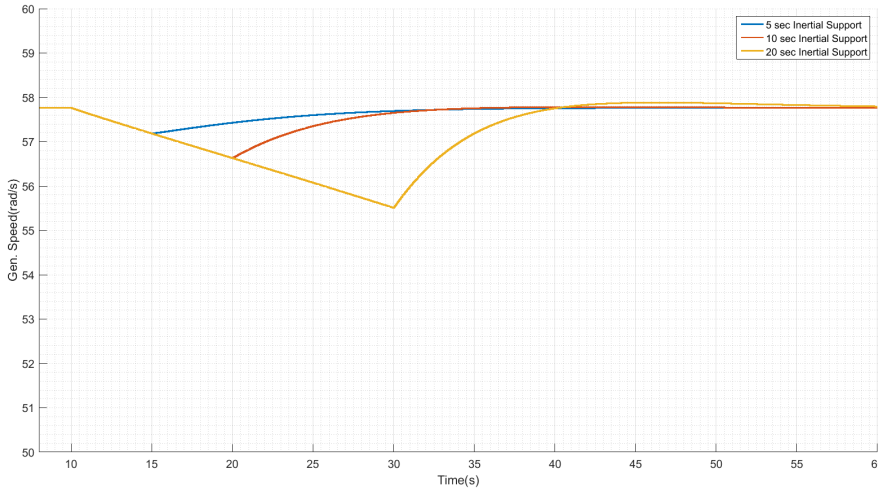


Figure 4.7: Generator Speeds of the Wind Turbine for Low Wind Scenario

torque for 20 second case is also shown in Fig. 4.9.

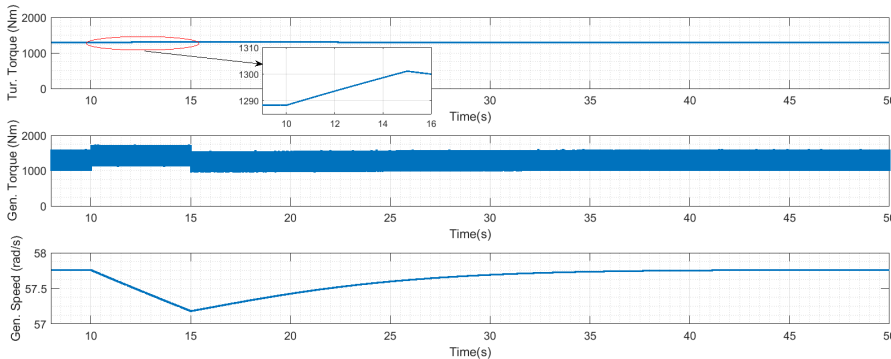


Figure 4.8: Turbine Torque, Generator Speed and Torque for 5 Seconds Support under Low Wind Speed

When the active power is increased, increased amount of active power is transferred from MSC to GSC. Increased active power should be injected to grid without causing excessive voltage rise on the DC-bus. It is to note that the voltage rise in the very first seconds in inertial support activation is same for all three support cases. However, the voltage drop will be highest in the 20 seconds case. DC-link voltage for 20 seconds support case is given in Fig. 4.10. The rise on DC-bus voltage can be considered as negligible for three support cases.

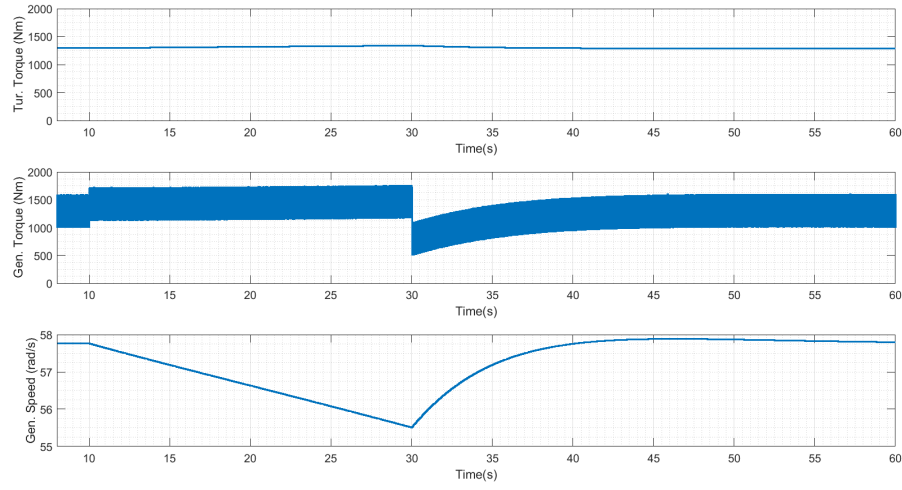


Figure 4.9: Turbine Torque, Generator Speed and Torque for 20 Seconds Support under Low Wind Speed

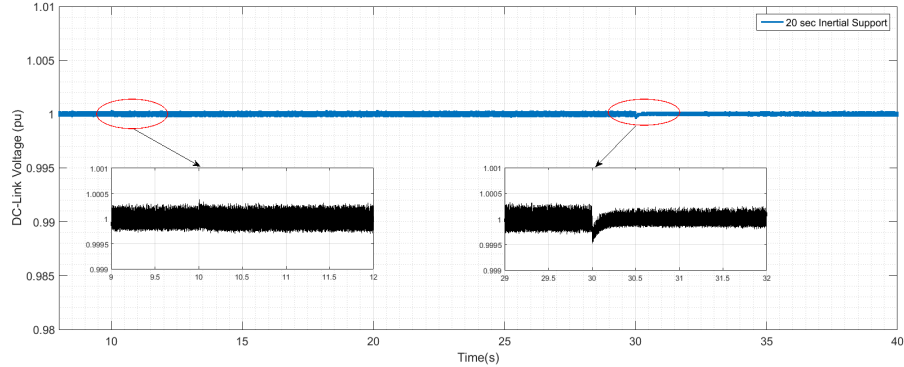


Figure 4.10: DC-Link Voltage for 20 Seconds Support in Low Wind Speed

4.2.2 Medium Wind Scenario

In the medium wind scenario, wind turbine operated in the middle of the generator speed range. The medium wind speeds have the huge potential for fast inertial support as stated in the Section 4.1. Besides, the wind turbine has more kinetic energy than that of low wind scenario and it can reach higher active power values due to its higher MPPT speed. The wind speed is selected as 6m/s in this scenario.

4.2.2.1 Fast Inertial Support Limit in Medium Wind Scenario

It is already mentioned that wind turbines in the medium wind speed scenario can increase its power more than that of low wind speed scenario. The reason is the dependency of the active power on the generator speed. The active power limit in the medium wind speed scenario is given in Fig. 4.11. The wind turbine active power is increased more than 0.4pu as expected in the Fig. 4.2.

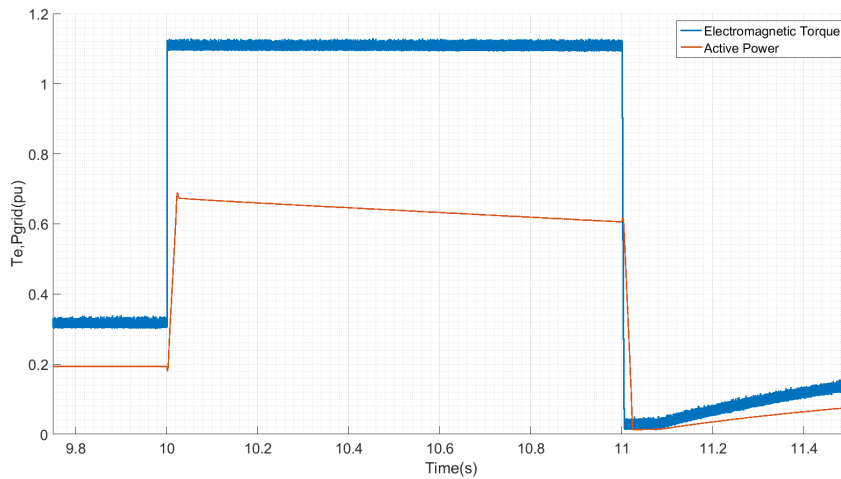


Figure 4.11: Fast Inertial Support Active Power Limit for Medium Wind Scenario

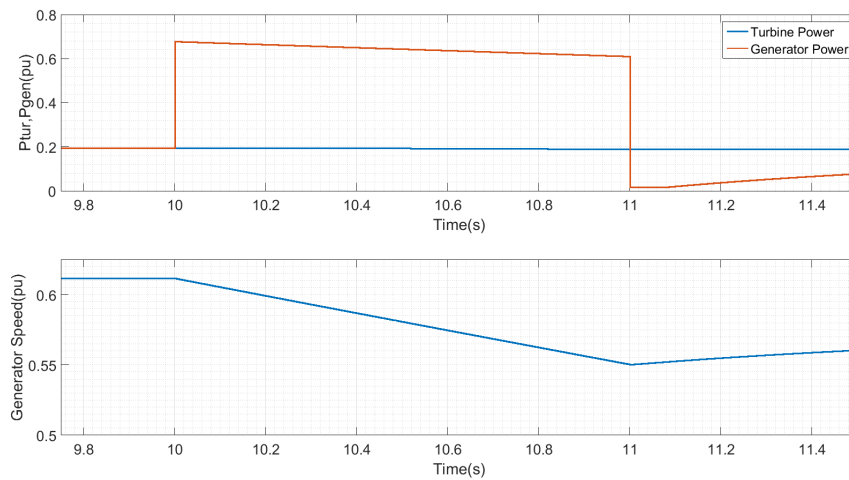


Figure 4.12: Generator and Turbine Power and Generator Speed for Medium Wind Speed Limit Case

The generator and turbine powers as well as generator speed are depicted in Fig. 4.12. Generator speed decreases due to increased generator power while the turbine power is almost constant. Since the turbine leaves the MPP point, the turbine power declines. However, the change in the turbine power is small. Therefore, the turbine power is said to be constant for this interval. The variation of the DC-bus voltage is shown in Fig. 4.13. The rise in the DC-link voltage is up to 1.04pu and it is regulated in 200ms.

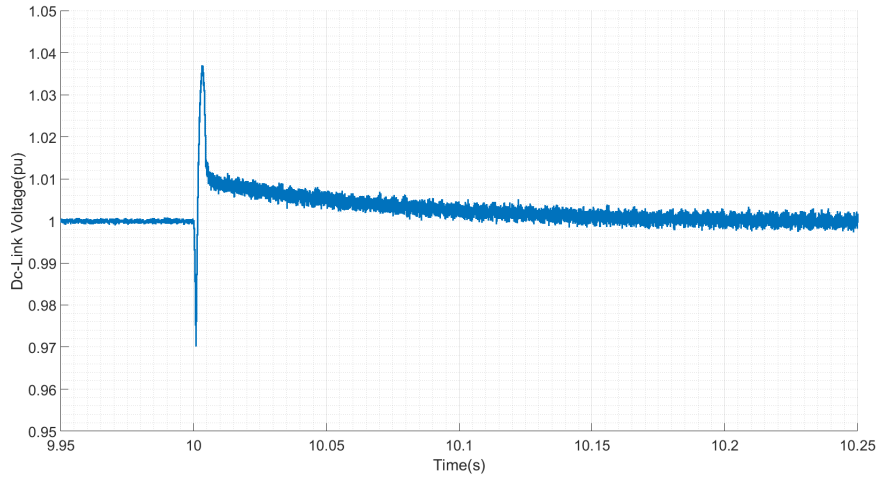


Figure 4.13: Variation of DC-bus Voltage for Medium Wind Speed Limit Case

4.2.2.2 Moderate Fast Inertial Support for in Medium Wind Scenario

Fast inertial support with a duration of 1 second can be evolved to moderate inertial support with longer duration of support and small increase in active power. Therefore, the active power of the wind turbine is increased by 10% and it is shown in Fig. 4.14 for three different time intervals. The recovery period of shortest support case is much more smoother than the longer ones. When the support time is increased, active power of the wind turbine is almost halved that might cause also problems in frequency stability of the power systems.

In medium wind scenario, higher support time causes decreased active power after the support. The reason is the lower speed value obtained with higher support time. Generator torque is decreased much higher for this case in order to recover the speed.

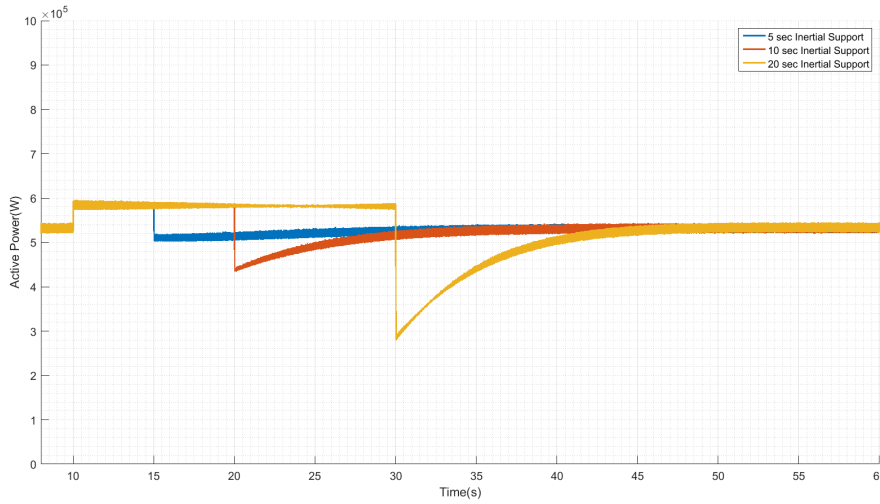


Figure 4.14: Active Power Output of the Wind Turbine for Medium Wind Scenario

The generator speed, turbine and generator torques are shown in Fig. 4.15. After the support, MPPT algorithm takes action and regulates the speed correspondingly. Therefore, the generator torque jumped down to lower value to restore the MPPT speed. The negative jump in generator torque creates a negative jump in the active power of the wind turbine since the transferred power is the multiplication of generator torque and generator speed.

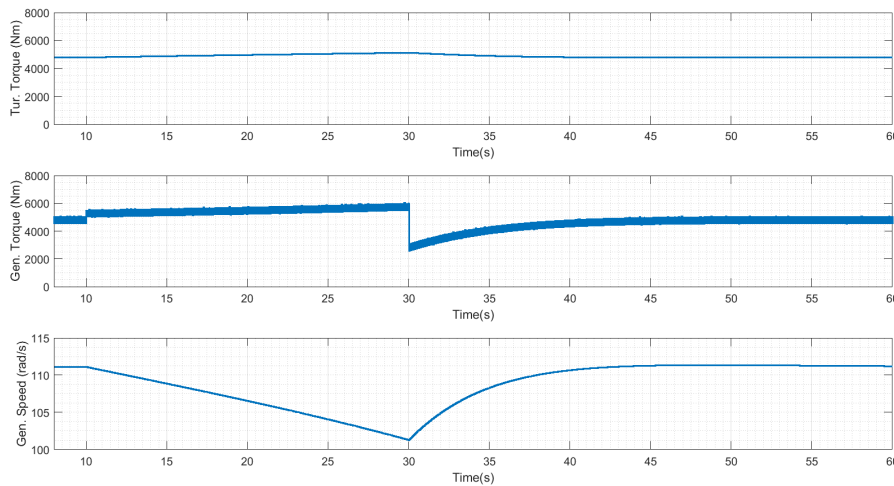


Figure 4.15: Generator Speed, Generator and Turbine Torques for Medium Wind Scenario for 20 Seconds Support

The fast inertial support is activated in time 10 seconds. The rise on the DC-bus voltage is negligible as in the case of low wind scenario. However, the voltage drop at the end of support is much more significant than that of low wind scenario. The variation of DC-bus voltage with inertial support is shown in Fig. 4.16 for the 20 seconds support case.

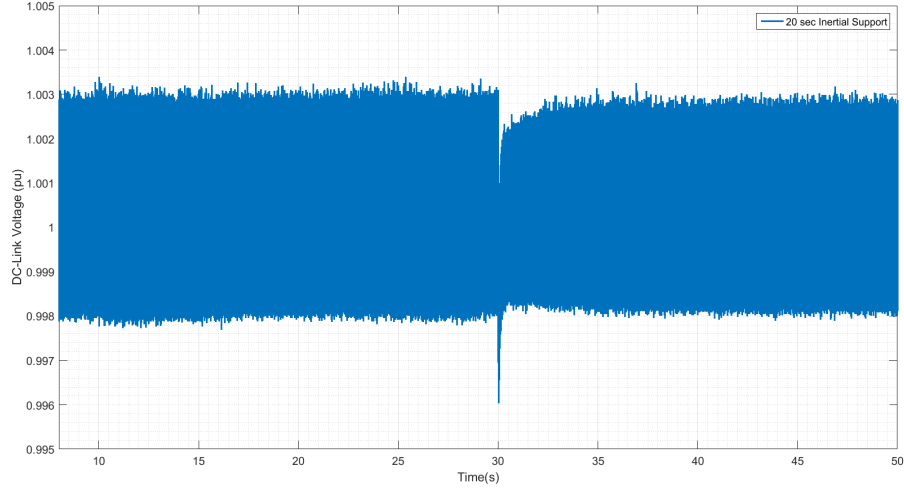


Figure 4.16: DC-Link Voltage for 20 Seconds Support in Medium Wind Speed

4.2.3 High Wind Scenario

In this section, wind turbine operation with high wind speed is investigated. The high wind scenario is much different than the low and medium wind speed scenarios. Firstly, the wind turbine injects its maximum power to grid. Secondly, the generator reference speed is the maximum allowable speed, ω_{max} which implies that wind turbine operation is away from MPPT operation. In order to keep the generator in the maximum available speed, the pitch angle is used in order to curtail wind power. The reason for using pitch angle is that the generator torque is limited by T_{P-lim} . Therefore, the wind turbine decreases turbine power and torque by increasing pitch angle. The wind speed in this scenario is selected as 11.4m/s.

4.2.3.1 Fast Inertial Support Limit in High Wind Scenario

Wind turbines are able to provide inertial support in high wind speed as long as converter power rating is higher than the wind turbine generator power rating. The wind turbine investigated throughout the study has a converter rating of 3.04MVA meanwhile turbine power rating of 2.75MW. Therefore, active power output can be increased up to 3.04MW during support interval as long as the converter and generator handle excess losses due to overloading. Otherwise, wind turbine cannot provide inertial support for high wind speeds. In the low and medium wind scenarios, the active power can be increased much higher than 10% in the limit case. However, the limit and moderate fast inertial support cases are the same for high wind speed scenario and limited by 10%. The active power is increased to its limit for 1 second duration as shown in Fig. 4.17. The generator torque is increased from 1pu to 1.1pu. The increase in the torque rises the power to the maximum allowed power rating. However, the increase in the currents causes excess heat and mechanical stress on the wind turbine generator, gearbox and the power converters. Therefore, the support period should be limited as well as the next possible support should be delayed.

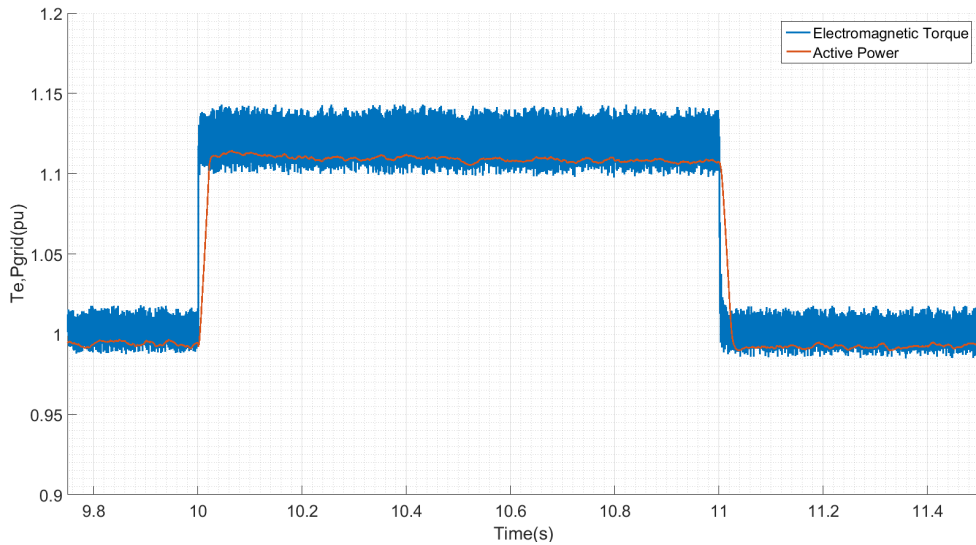


Figure 4.17: Fast Inertial Support Active Power Limit for High Wind Scenario

Turbine and generator powers, generator speed and pitch angle is shown in Fig. 4.18. The turbine power in this case rises with the inertial support that is different than low and medium wind scenarios. Moreover, the speed starts decreasing with the support.

However, as the generator speed declines below the maximum generator speed, pitch angle of the turbine blades decreases. Therefore, the fast inertial support does not require speed recovery since the speed is recovered as soon as the power goes back to pre-disturbance value.

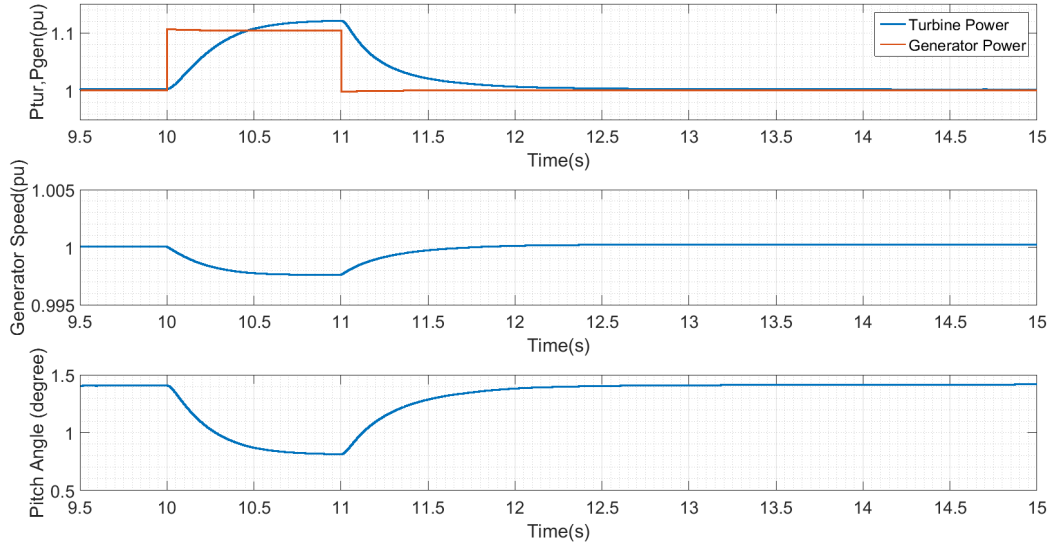


Figure 4.18: Turbine and Generator Powers, Generator Speed and Pitch Angle for High Wind Limit Scenario

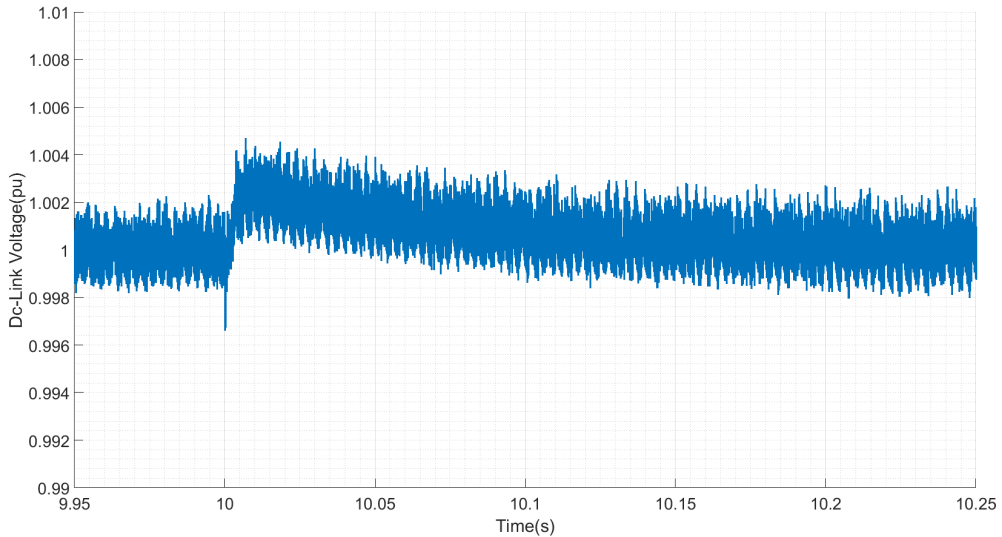


Figure 4.19: Variation of the DC-bus Voltage for High Wind Limit Scenario

Finally, the DC-bus voltage is shown in the Fig. 4.19. The reason of the rise on DC-bus is the unbalance between generator power and power injected to grid. In

other words, rise on the DC-bus voltage is directly linked to the additional power. The quicker the grid power is increased, the lower DC-bus voltage rise is obtained. Since the increase in the active power to the limit is lowest in the high wind scenario, DC-bus voltage rise is lower than that of the low and medium wind scenarios.

4.2.3.2 Moderate Inertial Support Limit in High Wind Scenario

In this part, the active power of the wind turbine is increased again by 10% with three different time intervals. The active powers are shown in Fig. 4.20.

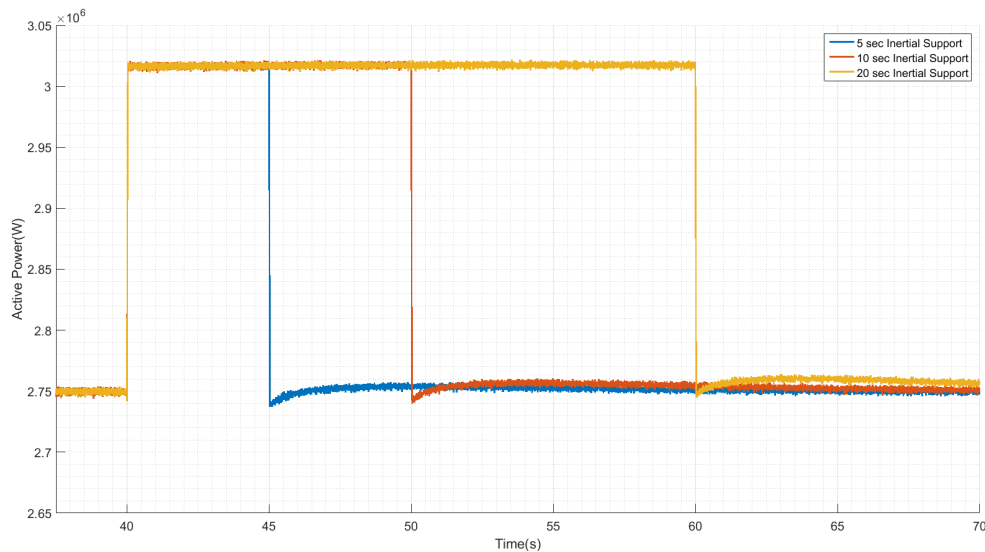


Figure 4.20: Active Power Output of the Wind Turbine for High Wind Scenario

An interesting observation in high wind scenario is that there is no speed recovery process. As soon as the speed is decreased, the pitch controller decreases the blade angle which causes an increase in turbine torque. Therefore, in this case, turbine power decreases back to normal rather than a lower power value as in the other scenarios. In the high wind scenario, the generator torque hits the limit defined for normal operating conditions. This is why generator speed is regulated with the help of blade angle. Therefore, pitch angle is also important in this section.

Generator speed, turbine and generator torques as well as pitch angle for 20 seconds support case is shown in Fig. 4.21. Generator speed starts decreasing when the generator torque is increased. However, the pitch controller decreases the blade angle

since the generator speed is below the maximum speed. Therefore, the generator speed rises when the pitch angle is decreased. Note that pitch servo acts slower than the generator torque increase time. This is why the generator speed decreases until the pitch angle is decreased. Generator speed might not be disturbed if the pitch controller is able act fast enough.

After the generator speed is arrested by the pitch angle decrease, generator speed rises towards the maximum generator speed. If the support time is increased, the generator speed will reach the maximum speed, and will stay constant with a new pitch angle. This means that the turbine is able to provide the support forever. However, the full capacity of the converter cannot be used permanently since it causes overloading of the converters in the wind turbine and excess heat losses. Therefore, maintaining permanent support would be dangerous. Finally, the rise on the DC-bus voltage is the same with the high speed limit case meanwhile the voltage drop at the end of the support period might increase with the duration. Nonetheless, the detailed modelling of the DC-bus voltage with the actual converter parameters would give the most realistic results for this study.

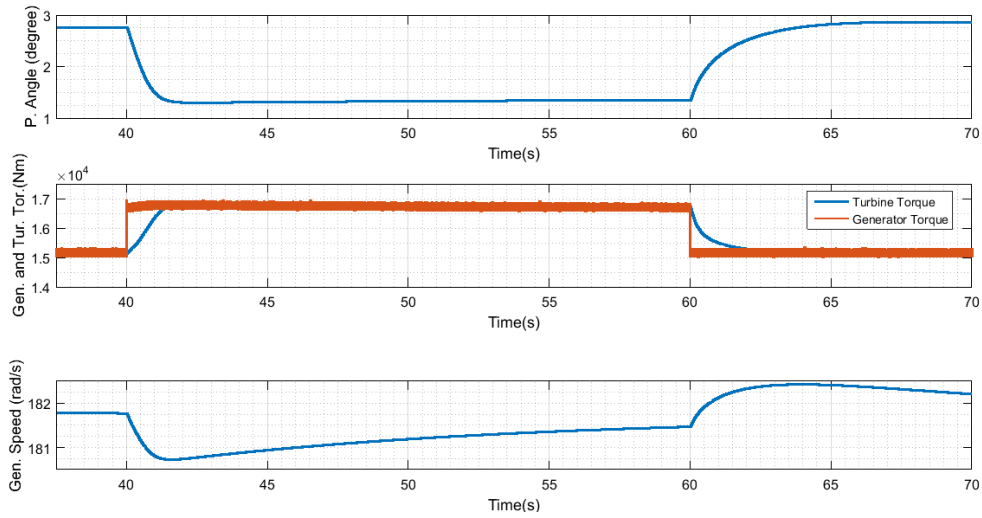


Figure 4.21: Pitch Angle, Generator Speed, Generator and Turbine Torques for High Wind Scenario for 20 Seconds Support

4.3 Probabilistic Approach for Fast Inertial Support

In the Section 4.1, the inertial support limits are investigated for different wind speeds. It is stated that the wind turbines can increase their active power outputs by highest amounts in the low and medium wind speeds. In order to increase the meaningfulness of such support, probability of different wind speeds is studied. Wind speed measurements used in this thesis are taken from a real wind farm with GE 2.75-103 model wind turbines between 01/01/2017 and 21/08/2017. Probability density function (PDF) of the measurements is given in Fig. 4.22. The wind speed measurements have a mean of 7.13 with a standard deviation of 3.85.

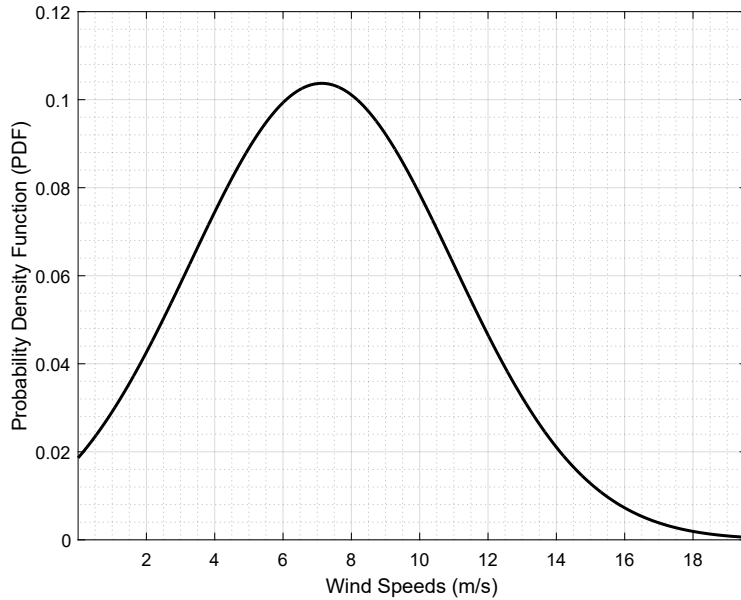


Figure 4.22: Probability Density Function of Measured Wind Speeds

For a defined wind speed, the active power increase can be calculated by considering the Section 4.1. However, likelihood of such an increase can be calculated by integrating PDF over desired the wind speed range. This can also be calculated from the cumulative distribution function (CDF) of the measurements. In this case, CDFs of the wind speed range limits will be used. Wind Speed CDF is given in Fig. 4.23.

By utilizing the wind speed measurements and the possible increase in the active output power, it is possible to define availability of the wind turbine for a possible

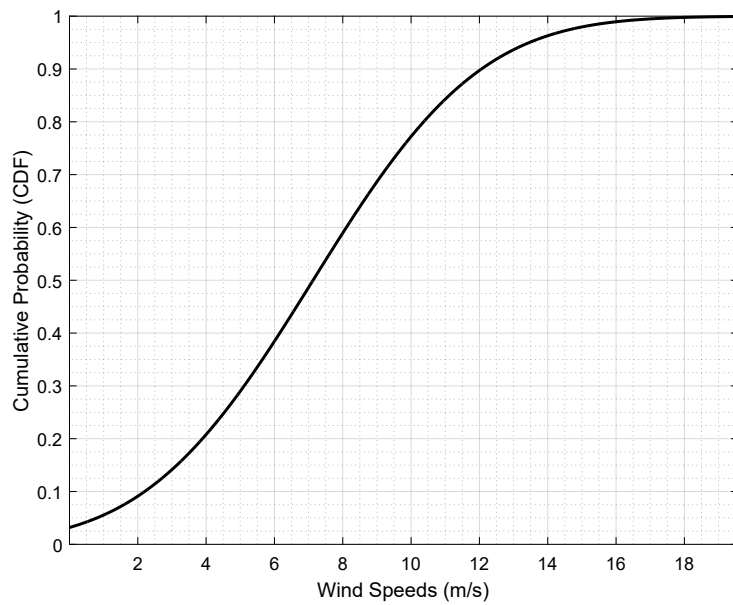


Figure 4.23: Cumulative Distribution Function of Measured Wind Speeds

inertial support. In other words, the increase in the active power can be united with the probability of the corresponding speed. In this way, the contribution from different wind speeds is obtained. The net power contribution for varying wind speed is given in the Fig. 4.24.

First of all, the net contribution when the wind speed is below 3m/s is zero since the turbine is in the cut-off. The probability of the cut-off according to wind speed measurements is found out as 14.16 from the pdf or cdf of the measurements. The main contribution concentrates inside the wind speed range between 3 and 10. Due to the fact that this wind speed range has both higher probability and higher increase capability, the main contribution is provided inside this range. Meanwhile, the higher speed range has relatively lower contribution due to its lower probability and lower capability.

Another important criteria is the net contribution from all wind speeds. Since Fig. 4.24 is basically product of the pdf given in Fig. 4.22 and the increase in the active power given in Fig. 4.2, the area under the graph gives the net contribution from a wind turbine by considering the probability of the each wind speed measurement. Therefore, it can be concluded that the wind turbine studied in this thesis subject is

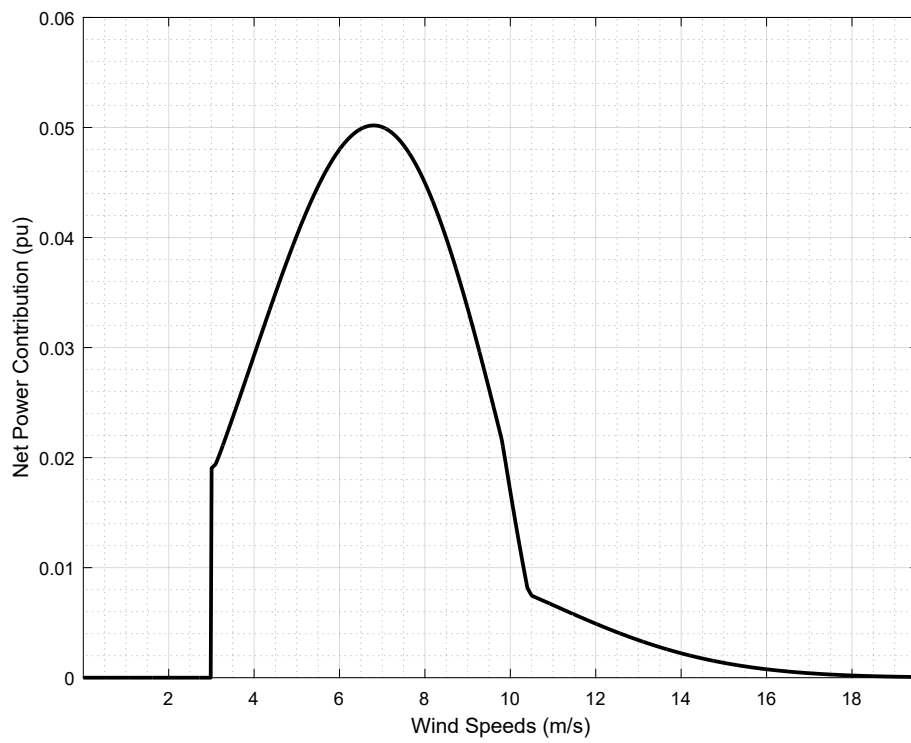


Figure 4.24: Distribution of Fast Inertial Support

able to provide 0.3pu active power.

CHAPTER 5

EFFECTS OF SYNTHETIC INERTIA IMPLEMENTATION

The concept of synthetic inertia or virtual inertia suggest a frequency response from renewable energy systems depending on the RoCoF of the electricity grid. As explained at the end of Chapter 3, a renewable energy system can provide an additional power according to the Swing Equation. In this chapter, the synthetic inertia implementation on a variable speed PMSG wind turbine is tested in P.M. Anderson 9 bus test case which is constructed in Matlab-Simulink environment. The test case is subjected to an sudden load connection in the different scenarios.

5.1 P.M.Anderson 9 Bus Test Case

5.1.1 System Properties

In order to understand frequency dynamics better, P.M. Anderson test case has been used in the study. The single line diagram of the system is given in Fig. 5.1. The test case consists of three generators and three loads. Generators in the system are connected to 230 kV high voltage (HV) network with step-up transformers.

The biggest generator in the system is a hydro power plant with a power rating of 247.5 MVA. The remaining ones are steam generators. The power ratings of the generators are given in Table 5.1. The loads in the system are connected directly to the HV network. The active and reactive power ratings of the loads are listed in Table 5.2. System detailed properties are given in Appendix B.

Generators	Power Rating (MVA)	Plant Type
Gen 1	247.5	Hydro
Gen 2	192	Steam
Gen 3	128	Steam

Table 5.1: Generator Properties of Test System

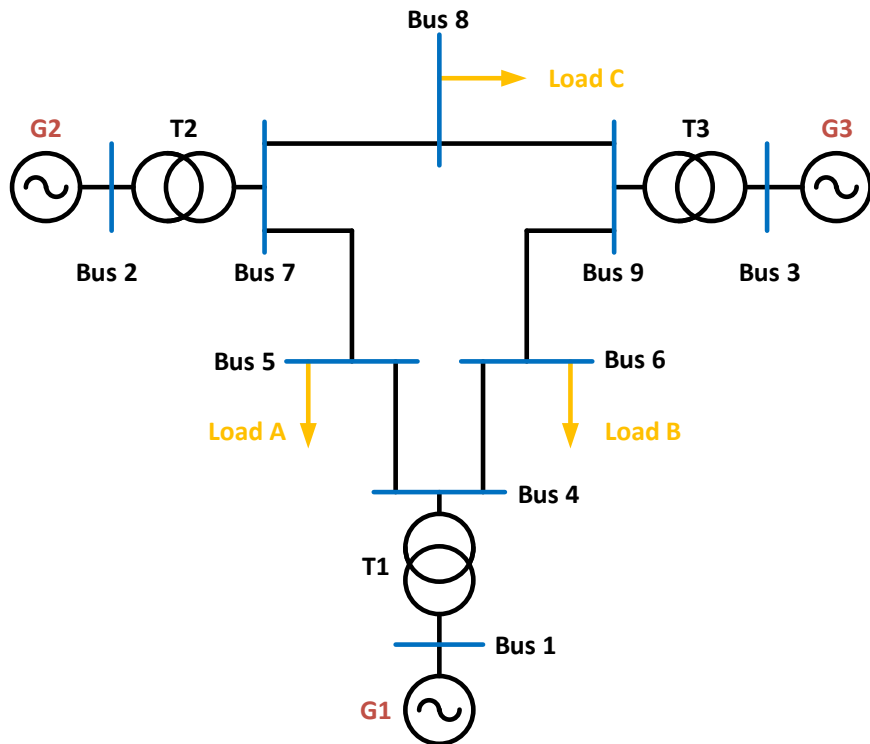


Figure 5.1: P.M.Anderson Test Case

Generators	Active Power (MW)	Reactive Power (MVar)
Load A	125	50
Load B	90	30
Load C	100	35

Table 5.2: Load Properties of Test System

5.1.2 Load Flow Analysis for Base Case

Successful grid operation requires a load flow analysis in order to ensure that bus voltages are inside the allowed band and power flows are below the power carrying capabilities of the lines. Load flow results are tabulated in Table 5.3.

Bus #	Bus Type	Voltage	Angle	Pg	Qg	Pl	Ql
1	SL	1.04	0	71.65	27.05	0	0
2	PV	1.025	9.28	163	6.65	0	0
3	PV	1.025	4.66	85	-10.86	0	0
4	PQ	1.0258	-2.22	0	0	0	0
5	PQ	0.9956	-3.99	0	0	125	50
6	PQ	1.0126	-3.69	0	0	90	30
7	PQ	1.0258	3.72	0	0	0	0
8	PQ	1.0159	0.73	0	0	100	35
9	PQ	1.0323	1.97	0	0	0	0

Table 5.3: Load Flow Results in Base Case

5.1.3 Base Case Frequency Response for Additional Load Connection

It is obvious that power system networks experience high RoCoF when either high amount of generation trips or high amount of load connects to system. These two main event can be used in the simulation to create frequency disturbances. Since the simulation in Simulink environment slows down with the increasing amount of generators, the disturbances are created with load connections.

System dynamical properties are listed in Table 5.4. Power generation references are determined based on the load flow of powergui toolbox. Machine initialization toolbox is also used to initiate the state of generators in the system. However, the system does not start with the steady state. Still, system goes to steady state within a few seconds. Frequency of the network is disturbed with a load connection in the t=10 seconds in order to observe the frequency stability of the system. For 10% load

Total System Load	315 MW
Generator Droop Settings	5%
Stored Kinetic Energy at Nominal Speed	3.305 GWs
Gen 1 Inertia Constant	9.5515 s
Gen 2 Inertia Constant	3.9216 s
Gen 3 Inertia Constant	2.7665 s

Table 5.4: System Dynamical Properties

connection, a load of 31.5 MW is connected to system from Bus 6. Location of the additional load is depicted in Fig. 5.2.

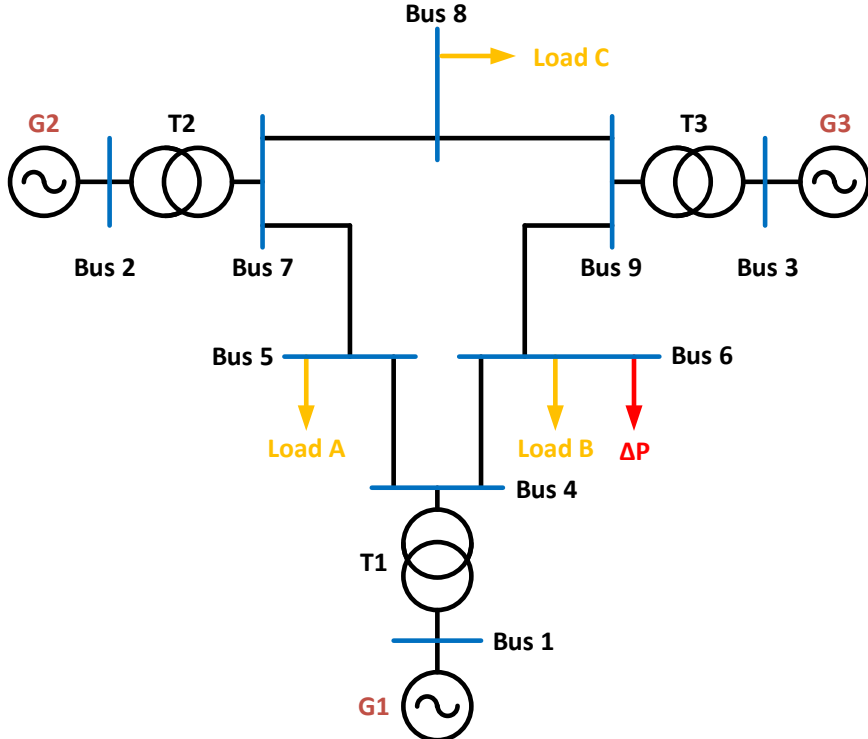


Figure 5.2: Location of the Additional Load

According to the 10% load connection to system, generator frequencies are shown in Fig. 5.3. As it can be seen from Fig. 5.3, rotor swings exists in the frequencies. However, the frequency of generator 1 is the most smooth one due to its huge inertia constant. Meanwhile, the generator 2 and generator 3 follow the frequency of generator 1 with higher rotor swings.

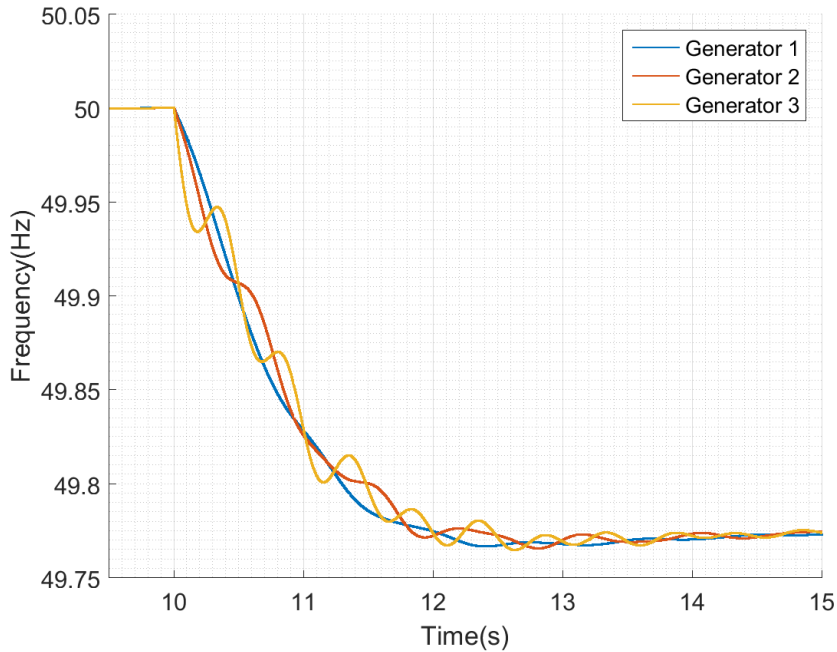


Figure 5.3: Generator Frequencies for 10% Load Connection

In the system, frequency of Bus 1 can be assumed as constant throughout the network since the system is small enough to assume a single frequency inside the network. This assumption can be verified by comparing the frequencies in Buses 1, 5 and 6. Fig. 5.4 shows the frequency of the generator 1 frequency as well as the load frequencies captured with Simulink PLL block. The only difference is the instant following the load connection. The sharp frequency decline delays the PLL loop to capture the frequency.

5.2 Modified Case

In order to observe the effect of the renewable energy penetration to grid, the P.M. Anderson test case is modified such that a wind farm consists of 20 wind turbine is connected to network. Since the transmission network of the test case is under-utilized, the location of the wind farm has no effect on the frequency disturbance. Hence bus 5 is selected as the location for wind farm connection. Modified system is depicted in the Fig. 5.5. In this case, generator 2 and 3 are still assigned to same power generation references meanwhile generator 1 decreases its generation since it

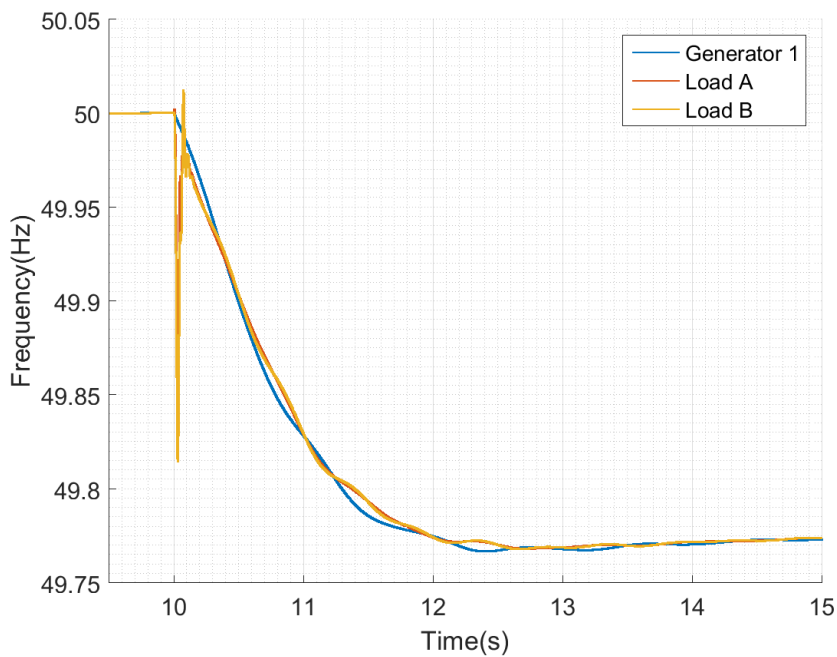


Figure 5.4: Frequencies in Generator 1, Load A and Load B

is the swing generator in the system.

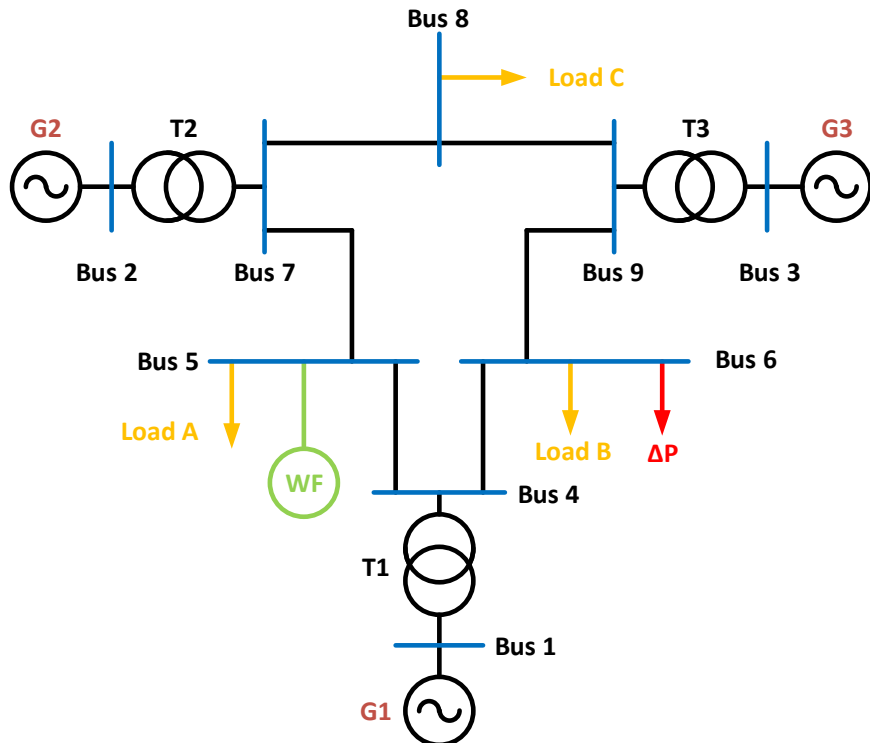


Figure 5.5: Modified System Single Line Diagram

5.2.1 Load Flow Analysis for Modified Case

Load flow analysis for modified case is listed in Table 5.5. The power injected from Bus 1 is decreased as expected. This can also be seen from the phase angle between 1 and 4. Phase angle difference between these buses decreased from 2.22° to 1.18° . Total power generation from active power from conventional generation units are also decreased. Therefore, the modified system resembles the base case with low power demand.

Bus #	Bus Type	Voltage	Angle	Pg	Qg	Pl	Ql
1	SL	1.04	0	38.06	25.07	0	0
2	PV	1.025	11.33	163	6.65	0	0
3	PV	1.025	6.32	85	-10.86	0	0
4	PQ	1.0263	-1.18	0	0	0	0
5	PQ	0.9995	-1.54	0	0	125	50
6	PQ	1.0128	-2.43	0	0	90	30
7	PQ	1.0266	5.77	0	0	0	0
8	PQ	1.0164	2.62	0	0	100	35
9	PQ	1.0326	3.62	0	0	0	0

Table 5.5: Load Flow Results for Modified Case

5.2.2 Modified Case Frequency Response for Additional Load Connection

The modified base is very similar to the Base Case except for a wind farm located in Bus 5. The renewable energy system in this case can be considered as a negative load. Therefore, base case with decreased load is under discussion in this subsection. The same amount of load is taken into operation at Bus 6 and the frequency response of the modified system is shown in Fig. 5.6.

Almost the same frequency response is observed in the system. The reason is that both systems have the same amount of stored kinetic energy. Another reason is that there is no congestion in the system due to under-utilized of transmission network. The

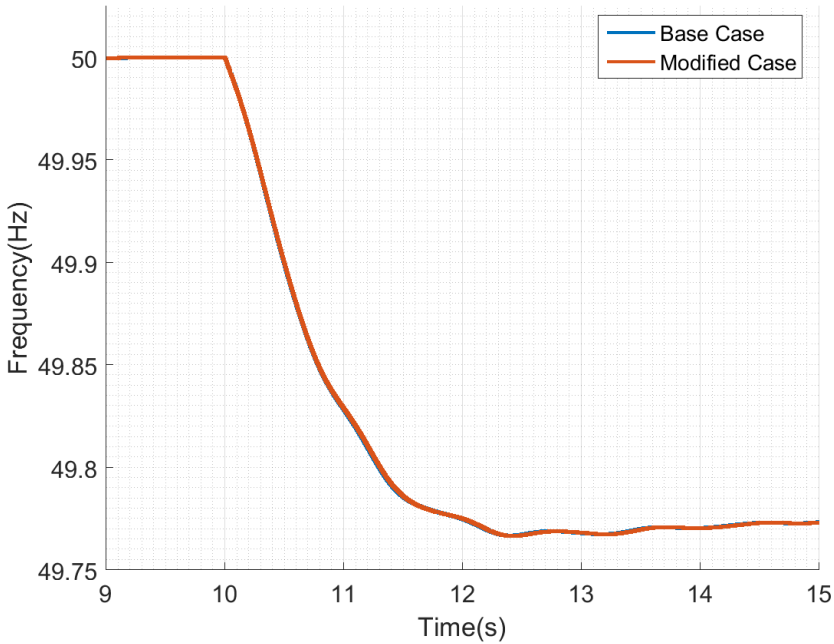


Figure 5.6: Comparison of Base Case and Modified Case Frequencies

same frequency response can also be observed in the rate of change of frequencies in Fig. 5.7. Almost the same RoCoF values are observed in the system. This concludes that renewable energy penetration does not change frequency response of the system if the only change in the system is the inclusion of renewable energy system. In other words, renewable energy systems does not affect the frequency response of the grid unless the system is replaced with a conventional generation unit. Note that the renewable energy systems are intermittent energy sources. However, in this study, the source of the renewable energy system is assumed as constant. Therefore, the reason of frequency disturbance is load connection rather than the change in active power output of renewable systems.

5.3 Decommissioned Case

As seen in the Modified Case, the frequency response of the system does not change with renewable energy inclusion. However, it is inevitable that renewable energy systems will replace the conventional units in future. In this case, the smallest generator, generator 3, will be decommissioned due to economical concerns. The decommis-

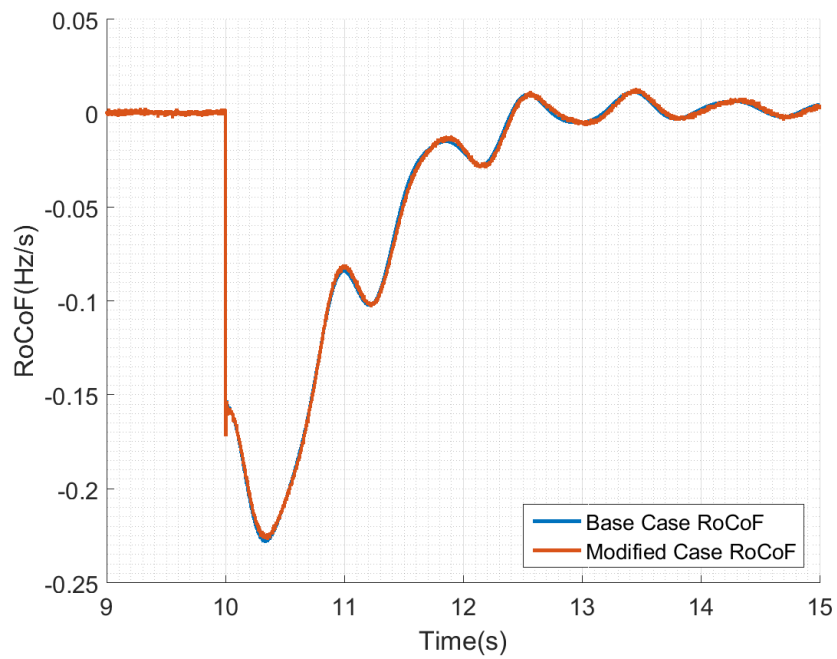


Figure 5.7: Comparison of Base Case and Modified Case Frequencies

sioned case diagram is shown in Fig. 5.8.

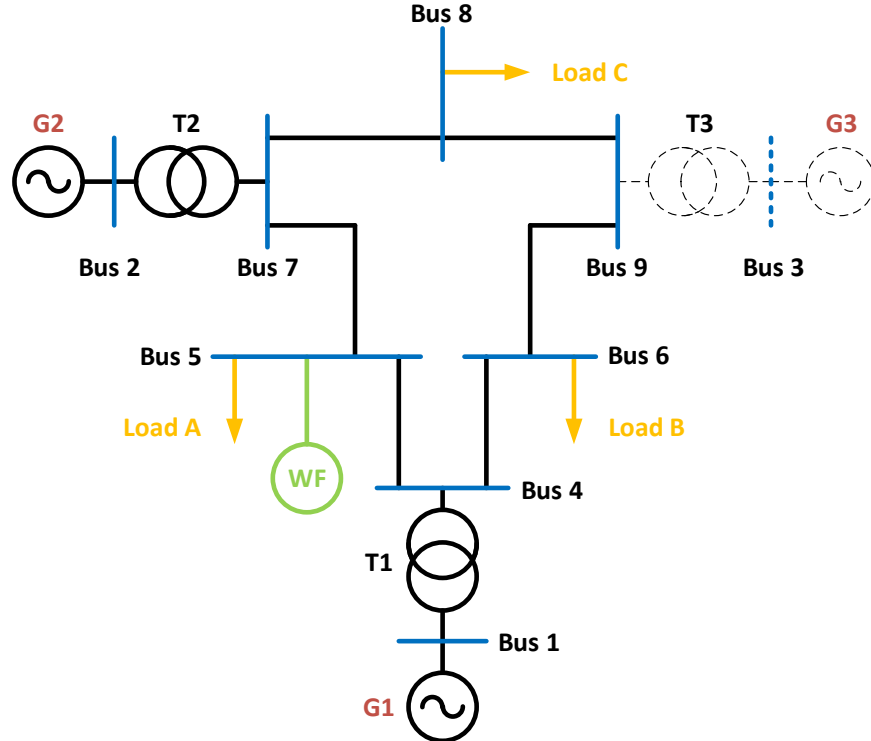


Figure 5.8: Decommissioned Case Single Line Diagram

Since the generator 3 is out of service, the stored kinetic energy is decreased in the system. Decommissioned system dynamical properties are updated and given in Table 5.6. Higher RoCoF value and lower frequency nadir are expected with the same additional load since the system dynamical properties are deteriorated with the removal of generator 3.

Total System Load	315 MW
Generator Droop Settings	5%
Stored Kinetic Energy at Nominal Speed	3.004 GWs
Gen 1 Inertia Constant	9.5515 s
Gen 2 Inertia Constant	3.9216 s

Table 5.6: System Dynamical Properties

5.3.1 Load Flow Analysis for Decommissioned Case

Since the generator 3 is out of service, generator 1 loading will be increased. Load flow analysis for decommissioned case is given in Table 5.7.

Bus #	Bus Type	Voltage	Angle	Pg	Qg	Pl	Ql
1	SL	1.04	0	121.76	16.26	0	0
2	PV	1.025	4.18	163	0.65	0	0
4	PQ	1.0332	-3.74	0	0	0	0
5	PQ	1.0083	-5.63	0	0	125	50
6	PQ	1.0224	-7.65	0	0	90	30
7	PQ	1.0294	-1.36	0	0	0	0
8	PQ	1.0207	-5.82	0	0	100	35

Table 5.7: Load Flow Results for Decommissioned Case

5.3.2 Decommissioned Case Frequency Response for Additional Load Connection

Decommissioned system is also subjected to the same frequency disturbance which is the additional load connection from Bus 6. System frequency response is observed and compared to Base Case and Modified Case in Fig. 5.9. The frequency response of the system gets worse with the generator 3 decommissioned. It results that the frequency nadir is decrease from 49.77Hz to 49.65Hz due to the decrease in the stored kinetic energy in the system. The deteriorated frequency response can also be seen from the comparison of RoCoFs that is given in Fig. 5.10.

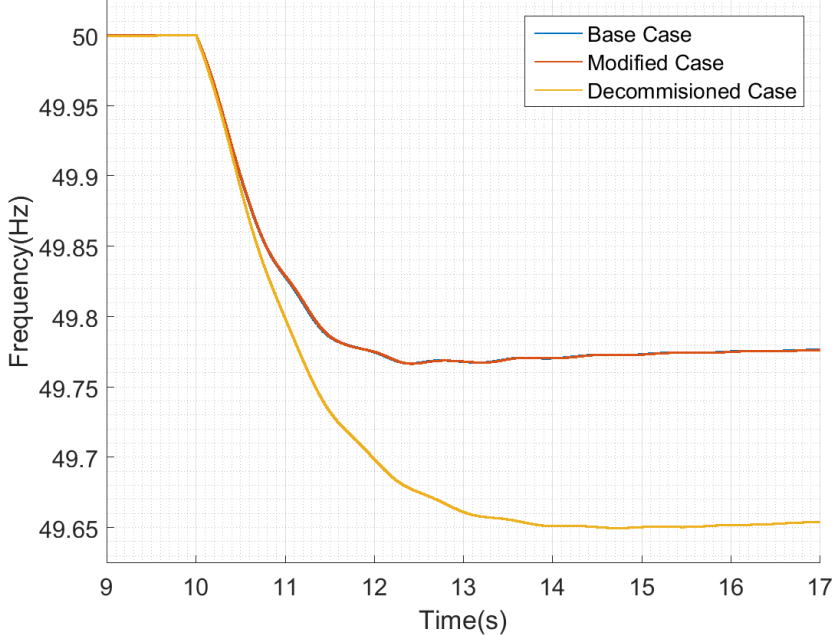


Figure 5.9: Comparison of Base Case, Modified Case and Decommissioned Case Frequency Responses

5.4 Modified Case with Synthetic Inertia

The frequency response of the modified system is investigated in Section 5.2 and the system frequency was almost the same with test system base case. However, the response of the system can be improved by provision of synthetic inertia. The

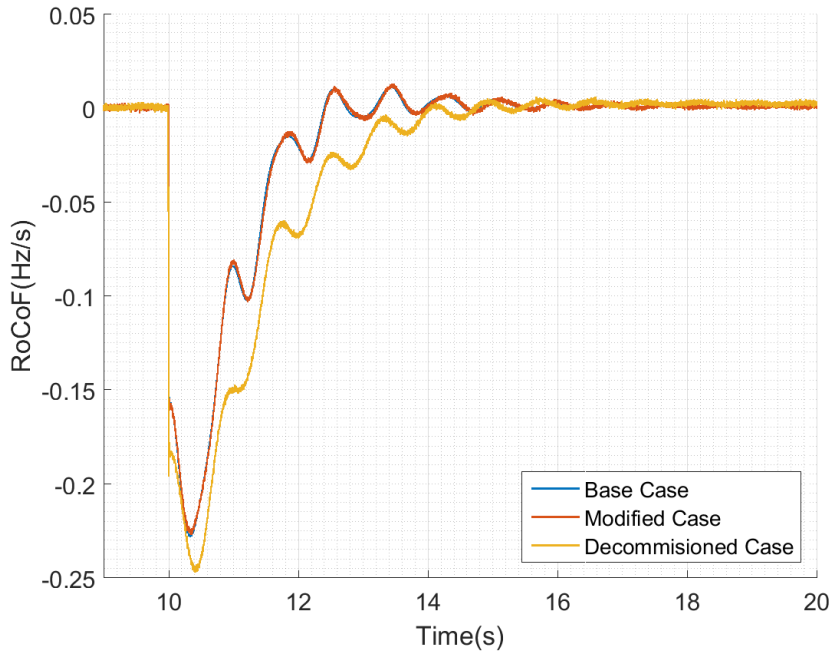


Figure 5.10: Comparison of Base Case, Modified Case and Decommissioned Case RoCoFs

wind turbines in the system is equipped with synthetic inertia that emulates inertia constants of 5s, 10s and 15s. The system response with inertial support provision is given in the Fig. 5.11.

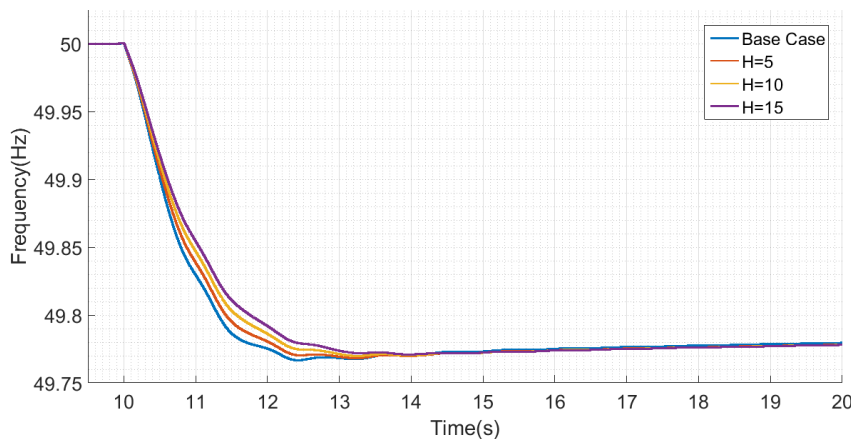


Figure 5.11: Emulation of the Different Inertia Constants for the Modified Case

Since the modified case frequency response is almost the same with the base case, the synthetic inertia implementation is improved the system frequency response. In other

words, the wind turbines are integrated to the system by emulating the synchronous generator behaviour. It is to note that huge amount of kinetic energy exists in the wind turbine systems. That stored energy can be utilized with the synthetic inertia method in order to improve frequency dynamics of the system.

Emulation of synchronous generator behaviour is basically increasing the amount of active power depending on the RoCoF of the grid and the inertia constant to be emulated. Since the higher inertia constant requires higher active power increase, the inertia constants of 10s and 15s result in better frequency dynamics. The frequency nadir of the base case is slightly increased. The effect of the synthetic inertia provision can also be observed in the system RoCoF values that is given in Fig. 5.12.

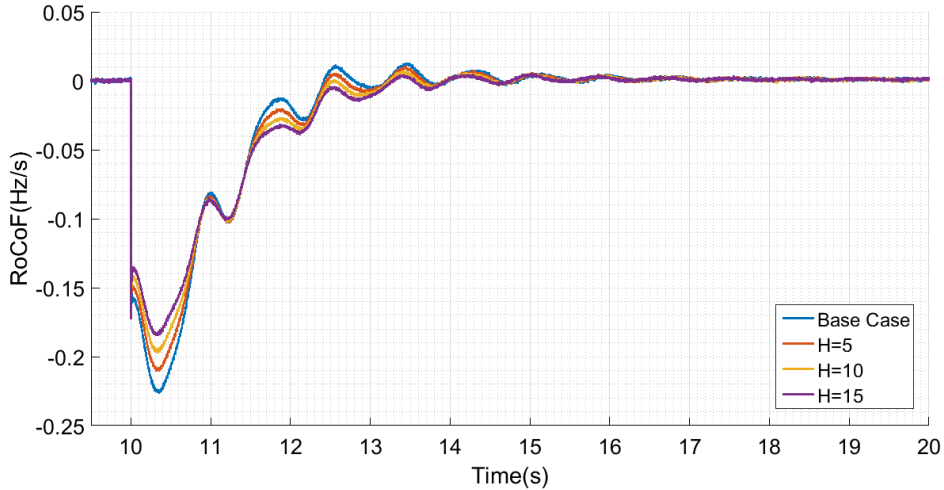


Figure 5.12: RoCoF of the Different Inertia Constants for the Modified Case

It is obvious that the base case experience the highest RoCoF in the very first second of the frequency disturbance. While the remaining cases is subjected to lower RoCoF at first, the base case RoCoF is the lowest following seconds. The reason is that the base case active power contribution in the first second is much higher than others. Hence, the case subjected to severe conditions react higher and faster resulting quick restoration of the system. Another observation is that all cases converges to the same steady state frequency due to the fact that inertial support affects the transient rather than the steady state values. The steady state frequency is dependent on the capacity of conventional synchronous generators and their droop constants. This is why the decommissioned case steady state frequency is lower than that of modified case.

5.5 Decommissioned Case with Synthetic Inertia

Decommissioned case frequency response for 10% additional load connection is studied in the Section 5.3. System frequency experiences high RoCoF and lower steady state frequency because of the removal of the generator 3. In this section, synthetic inertia method is implemented on the decommissioned case wind farm with different inertia constants. The resultant frequency responses are shown in the Fig. 5.13. As in the case of modified case, base case frequency response experiences steepest decline in the frequency meanwhile the higher inertia constant synthetic inertia implementations have smoother frequency decrease.

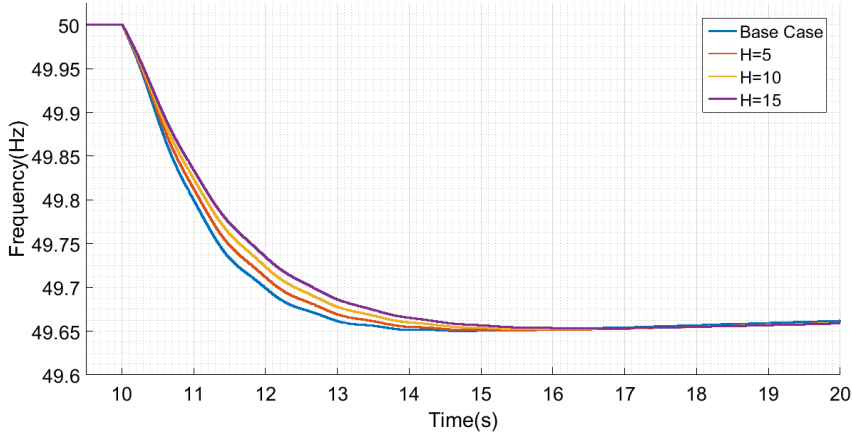


Figure 5.13: RoCoF of the Different Inertia Constants for the Decommissioned Case

The active power of the wind turbine for the different inertia constants is given in Fig. 5.14. It should be noted that the active power of the wind turbine is proportional with the RoCoF that is also given in Fig. 5.15. Note that 15s inertia constant is also emulated. It is stated that conventional generator inertia constants lie between 2-9s [4]. Nonetheless, synchronous generators have constant kinetic energy in the nominal frequency. However, the kinetic energy stored in the turbine inertia fluctuates with the generator speed. Moreover, wind turbine is able to emulate different inertia constant as soon as it has the capacity to increase its power. Even with the inertia constant of 15s, the wind turbine is far away from its maximum allowable power. Therefore, higher inertia constants can also be tested in the expense of longer speed recovery process whose resultant decreased power might also affect the RoCoF further.

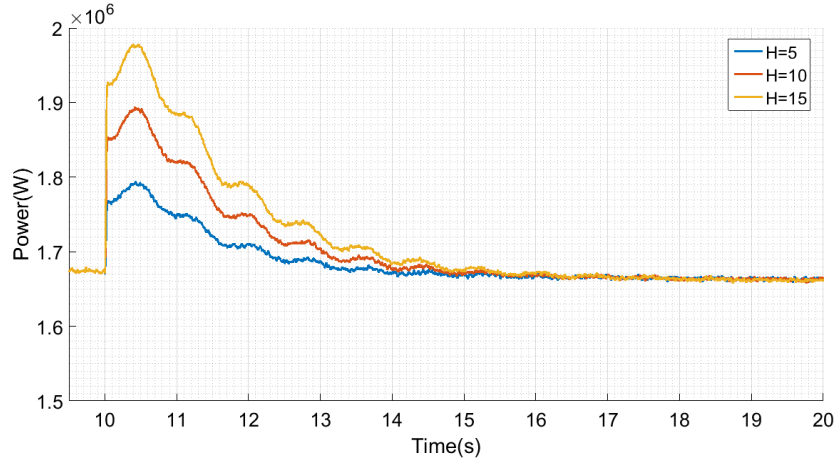


Figure 5.14: Wind Turbine Active Power for the Different Inertia Constants in the Decommissioned Case

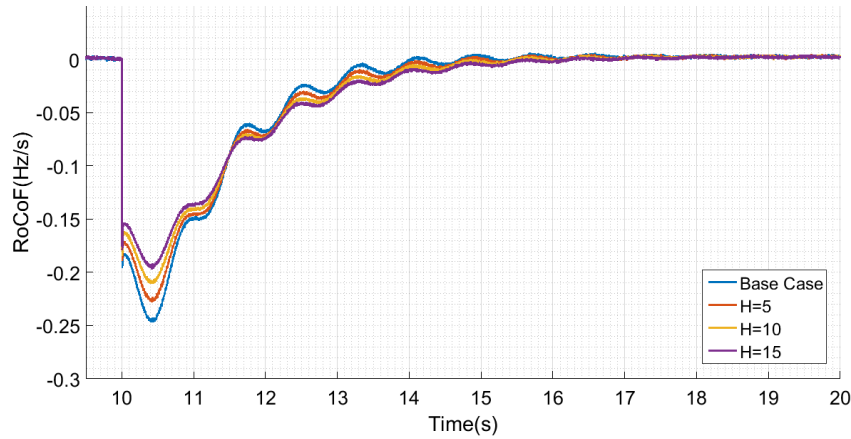


Figure 5.15: Wind Turbine Active Power for the Different Inertia Constants in the Decommissioned Case

5.6 Comparison of the Synthetic Inertia and Fast Inertial Support

In the Chapter 4, it is stated that the wind turbines have more than sufficient capacity in order to increase its active power. The fast inertial support concept is studied with different increase rates. The exaggerated inertial supports are studied to observe the turbine internal dynamics. In this section, the fast inertial support will be compared with the synthetic inertia. In other words, increasing active power by a defined percentage will be compared to a rise in the active power proportional to RoCoF. For this

reason, the same frequency disturbance is tested on the base case decommissioned case, the case where inertia constant of 10s is emulated and also the one with fast inertial support with 5% increased power by 5 seconds. Fig. 5.16 shows the variation of the active power. In order to increase the effectiveness of the fast inertial support, it is activated with a delay of 0.25s. In this interval, the synchronous generators take action for the upcoming disturbance. It should be underlined that the active power of the inertia emulated case is increased proportional to the RoCoF. Therefore, it declines as the RoCoF declines. Therefore, in the other half of the support time, it is below of the fast inertial support case. This phenomena can be clearly observed in the frequency response. It should be underlined that the swing equation is also used in fast inertial support recovery process in order to smooth recovery. This is why the active power of the both methods are the same in the recovery.

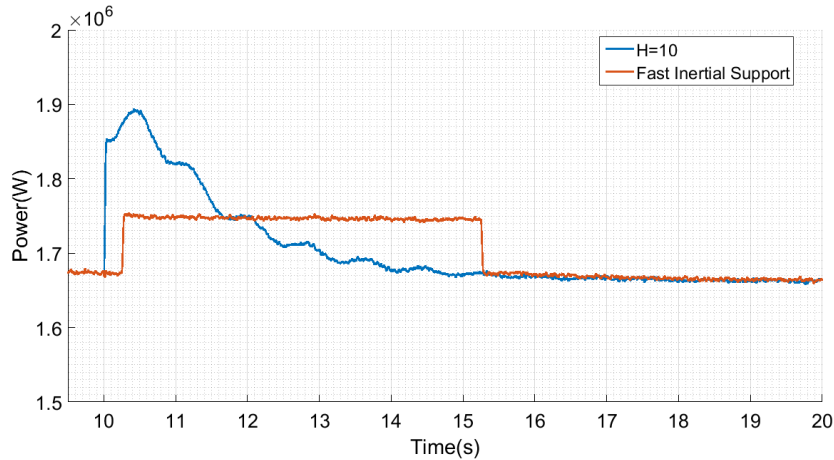


Figure 5.16: Comparison of the Frequency Responses for the Base, Fast Inertial Support and Synthetic Inertia Cases

The frequency response of these three cases is shown in Fig. 5.17. It is obvious that the base case frequency response has the poorest transient frequency. Besides, the synthetic inertia implemented case has the best transient behaviour for the very first seconds. Nonetheless, the fast inertial support case first converges to higher steady state frequency until the end of the support period. However, as soon as the support ends, the sharp decrease in the active power results a second dip in the frequency. The decrease in the active power can be considered as a second load connection to system. Therefore, the frequency is exposed to a second decrease at the end of support period

in fast inertial support implementation. In contrary, the synthetic inertia case active power is decreased down to lower values as the RoCoF is positive. Than means that the recovery process is already started inside the support. Hence, the secondary dip is not observed in this case.

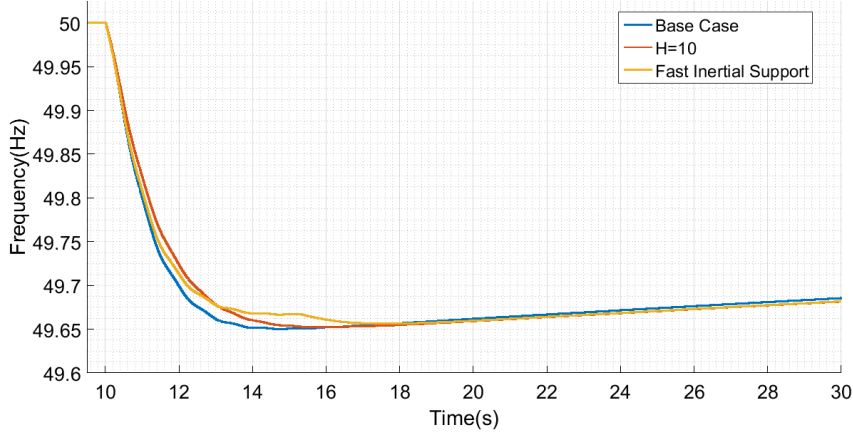


Figure 5.17: Comparison of the Active Power Increase in Fast Inertial Support Case and Synthetic Inertia Case

Finally, it should be noted that the energy extracted from wind turbine in the first 4 seconds are the same for both methods. However, synthetic inertia support utilizes that energy better by distributing the energy according to the RoCoF. Therefore, the grid takes the highest energy when it is needed most. But, the fast inertial support gives the same amount of energy for the support time. Besides, the additional power is cut suddenly that ruins the support. Hence, the fast inertial support needs to decrease the distribution of this energy according to some algorithms whose development is also out of scope of this study.

CHAPTER 6

EVALUATION OF FAST INERTIAL RESPONSE AND SYNTHETIC INERTIA IMPLEMENTATION

The installed capacity of power systems grows dramatically each passing day. Old fashion electricity grid is composed of conventional synchronous generators whose huge percentage is supplied from fossil fuels. Due to decrease the percentage of fossil fuel based generation, renewable energy systems which do not have environmental results are preferred and supported. Huge amount of renewable energy systems are connected to electricity grid during these two decades. Now, the debates try to answer whether electricity grid with only renewable energy systems are possible or not.

However, increase in the share of renewable energy in the installed capacity brought operational problems as well. As the total installed capacity grows, the rotational mass in the electricity grid slightly rises. This is due to the fact that installed PV systems do not have rotational bodies at all or wind turbines with full-scale power electronics does not effectively contribute the grid aggregated inertia. Hence, the power system with high renewable energy penetration is exposed to high RoCoF for the frequency disturbances. This implies that system will encounter unacceptable RoCoF values in frequency disturbances as long as the renewable penetration continues. Therefore, the upcoming future power system will require auxiliary services such as synthetic or virtual inertial support from all generation technologies that includes power electronics.

Renewable energy systems produces power according to the type of its power source. The input power is constant for an instant since the source (solar radiation, wind speed etc.) is constant. Therefore, the operation of renewable systems is different from the conventional power plants whose input power can be increased steadily by

the operator. Nonetheless, an additional energy source is required in the renewable systems that is stored kinetic energy in the wind turbine case. Therefore, the wind turbines are able to increase their active output power by extracting the kinetic energy stored in the turbine equivalent inertia. However, the amount of active power increase can be pre-defined values by fast provision as in the case of Chapter 4 or it can be proportional to RoCoF as in the case of Chapter 5.

6.1 Fast Inertial Support

Wind energy systems with full-scale power electronics can adjust its active power by controlling its output torque. Therefore, the active power can be quickly raised by extracting the energy in turbine inertia. However, the maximum value of the active power depends on the operating condition. Since the generator active power is also dependent on its speed, turbine power cannot be increased to rated power in low wind speeds. In high wind speeds, the active power before the support is already close to its rated value. Therefore, the increase in the active power is much more limited in high wind scenarios. In this study, fast inertial response in the medium wind speed is found out to have much more potential than the other scenarios. Besides, wind turbines can contribute better in low wind scenarios than that of high wind speed.

It is to note that the frequency disturbance occurs due to the unbalance between input mechanical power and output powers of the generators. Hence, the additional amount of active power that is provided from renewable energy sources in such instants is favourable. This is why the increase in the active power is much more important than the final active power amount. Therefore, knowledge of active power limits reveals the potential of variable speed wind turbines in order to contribute the frequency stability of the power systems.

Fast inertial response can be provided in different amount of time durations. Since the larger amount of support might result in higher speed deviations, the support time might be decreased. In contrary, higher support durations can be achieved with lower amount of fast inertial response.

Fast inertial response in this study is not a direct function of the RoCoF as in the case

of synthetic inertia implementation. However, an RoCoF indexing can be constructed for fast inertial support provision. The indexing scheme requires a RoCoF threshold and different RoCoF intervals. The highest RoCoF interval corresponds to the most severe frequency disturbances case and requires the highest amount of fast inertial support release with highest available support time. The higher energy extraction might even result in the stall of the turbine. Nonetheless, critical instant following the disturbance is much more important than the turbine speed recovery. Meanwhile, the lowest RoCoF interval would be assigned to lowest inertial support release with time duration in order not to result higher speed deviation.

6.2 Synthetic Inertia Implementation

Even though wind turbine power can be changed as desired inside an allowable power range, the fastest release of the power is not a solution for the power system network. Although huge amount of power is released in the disturbances, the restoration of that energy to the turbine causes further problems to grid. Therefore, the increase amount should be in coordination with the grid frequency behaviour. This is ensured with the synthetic inertia implementation in the Chapter 5. By adjusting active power according to the RoCoF of the grid, the active power is increased or decreased depending on the grid status.

The P.M. Anderson test case constructed in Matlab-Simulink environment is first tested with a load connection to see the frequency response of the system. The constructed system frequency falls at least for 2 seconds until the conventional generators increase their active power output. Frequency of the three generators are observed for the disturbance. In the system, generator 1 has the biggest inertia constant. Therefore, when the frequency of the system falls, there are rotor swings between generator 2 and 3 that follows the frequency of the generator 1. In the modified case, a wind farm with 20 wind turbines is connected to system in Bus 5. The wind farm connection does not change the generator 2 and 3 reference values but the generator 1 production. When the modified system is subjected to the same frequency disturbance, the system frequency response is not affected at all. The reason is that the test system has exactly the same kinetic energy or the effective inertia. Inertia existing in the wind farm does

not contribute the system frequency stability. Meanwhile the wind farm production can be considered as negative load whose power is not dependent on the frequency of the system.

The common concern in the frequency stability reports is not the renewable energy penetration itself but the renewable energy penetration that replaces the conventional synchronous generators. System frequency stability is subjected to change especially renewable energy systems are preferred over the conventional generation units. Therefore, the system frequency response gets more critical when a unit is decommissioned in the economical dispatch. To investigate this issue, the generator 3 is taken off from the system. Therefore, kinetic energy in the system declined that increased the responsibility of the remaining generators in the system. The test system in the decommissioned case is exposed to lower RoCoF and lower post-disturbance frequency. The reason in the lower RoCoF is the decreased rotational energy in the system i.e. lower inertia. Moreover, the lower post-disturbance is caused by the decreased primary reserve due to the generator 3 outage.

The most important feature of the synthetic inertia implementation is the RoCoF dependency of the support. The support in this method does increase and decrease the power value according to the pre-disturbance value. For instance, the power is above the pre-disturbance power value when the RoCoF is negative. In contrast, the lower amount of power injected to grid as soon as the RoCoF is positive. In this way, turbine recover its speed by injecting lower power to grid.

The synthetic inertia implementation is used for improving the transient behaviour of the frequency. In the literature variety of inertia constants are emulated in variable speed wind turbines. However, the emulated inertia constant are generally inside 2 and 10. Nonetheless, it is observed that the wind turbines have enormous capacity to increase their power. Therefore, in this study inertia constants more than 10s are also tested. However, further increasing inertia constants to be emulated would extract high amount of active power which increases the restoration time. Since the wind speed would not be constant for long time, increased inertia constants might cause problems.

6.3 FUTURE WORK

- Fast inertial support implementation has huge potential to increase the active power. However, as soon as the support ends, the decrease in the active power resembles a second load connection to system. Therefore, the system is exposed to a secondary decrease in the frequency. This is why the amount of additional power should be adjusted according to the grid requirements. Hence, a support index can be developed to reshape the fast inertial support.
- Fast inertial support in this study is activated according to the RoCoF threshold of 0.1Hz/s. However, the increase percentage is not a function of the grid parameters. Thus, an index might be constructed for the on-line employment of the fast inertial support. The index to be constructed will determine the increase percentage based on the pre-determined values.
- The effects of the fast inertial support on the DC-link voltage might be better investigated with more realistic modelling. The effectiveness of the new modelling might be tested in the wind turbine emulators.
- When the support is required in the high wind speeds, support power might hit the maximum allowed converter powers. The extra heat and mechanical stresses might also be tested in wind turbine emulators.

REFERENCES

- [1] Eurostat, “Renewable energy in the EU-newsrelease,” Tech. Rep. January, 2018.
- [2] European Commission; and IRENA International Renewable Energy Agency, “Renewable Energy Prospects for the European Union,” Tech. Rep. February, 2018.
- [3] IRENA, “A Renewable Energy Roadmap,” Tech. Rep. June, 2014.
- [4] P. Kundur, *Power System Stability and Control*. McGraw-Hill, Inc.
- [5] J. H. Eto, J. Undrill, P. Mackin, R. Daschmans, B. Williams, B. Haney, R. Hunt, J. Ellis, H. Illian, C. Martinez, M. O’Malley, K. Coughlin, and K. H. LaComare, “Use of Frequency Response Metrics to Assess the Planning and Operating Requirements for Reliable Integration of Variable Renewable Generation,” Tech. Rep. December 2010, Lawrence Berkeley National Laboratory (LBNL), Berkeley, CA (United States), dec 2010.
- [6] International Renewable Energy Agency (IRENA), *IRENA (2018), Renewable capacity statistics 2018*. 2018.
- [7] International Renewable Energy Agency, *Renewable Energy Statistics 2017*. 2017.
- [8] European Commission, “Communication from the Commission to the European Parliament, the Council, the European economic and social Committee and the Committee of the Regions - 20 20 by 2020 - Europe’s climate change opportunity,” *COM (2008) 30 final*, p. Brussels, 2008.
- [9] European Parliament, “Directive 2009/28/EC of the European Parliament and of the Council of 23 April 2009,” *Official Journal of the European Union*, vol. 140, no. 16, pp. 16–62, 2009.
- [10] REN21, *Renewables Global Futures Report*. 2017.

- [11] H. Klinge Jacobsen and E. Zvingilaite, “Reducing the market impact of large shares of intermittent energy in Denmark,” *Energy Policy*, vol. 38, no. 7, pp. 3403–3413, 2010.
- [12] M. Zipf and D. Most, “Impacts of volatile and uncertain renewable energy sources on the German electricity system,” *International Conference on the European Energy Market, EEM*, 2013.
- [13] A. Ipakchi and F. Albuyeh, “Grid of the future,” *IEEE Power and Energy Magazine*, vol. 7, no. 2, pp. 52–62, 2009.
- [14] D. Gautam, L. Goel, R. Ayyanar, V. Vittal, and T. Harbour, “Control strategy to mitigate the impact of reduced inertia due to doubly fed induction generators on large power systems,” *IEEE Transactions on Power Systems*, vol. 26, no. 1, pp. 214–224, 2011.
- [15] E. Muljadi, V. Gevorgian, and M. Singh, “Understanding Inertial and Frequency Response of Wind Power Plants Preprint,” *2012 IEEE Power Electronics and Machines in Wind Applications (PEMWA)*, no. July, pp. 1–8, 2012.
- [16] J. Van De Vyver, J. D. M. De Kooning, B. Meersman, L. Vandeven, and T. L. Vandoorn, “Droop Control as an Alternative Inertial Response Strategy for the Synthetic Inertia on Wind Turbines,” *IEEE Transactions on Power Systems*, vol. 31, no. 2, pp. 1129–1138, 2016.
- [17] G. Lalor, J. Ritchie, S. Rourke, D. Flynn, and M. O’Malley, “Dynamic frequency control with increasing wind generation,” *IEEE Power Engineering Society General Meeting, 2004.*, pp. 1–6, 2004.
- [18] J. Ekanayake, “Control of DFIG wind turbines,” *Power Engineer*, vol. 17, no. 1, pp. 28–32, 2003.
- [19] J. Ekanayake and N. Jenkins, “Comparison of the response of doubly fed and fixed-speed induction generator wind turbines to changes in network frequency,” *IEEE Transactions on Energy Conversion*, vol. 19, no. 4, pp. 800–802, 2004.
- [20] J. Morren, S. de Haan, W. Kling, and J. Ferreira, “Wind Turbines Emulating Inertia and Supporting Primary Frequency Control,” *IEEE Transactions on Power Systems*, vol. 21, no. 1, pp. 433–434, 2006.

- [21] J. Morren, J. Pierik, and S. W. de Haan, “Inertial response of variable speed wind turbines,” *Electric Power Systems Research*, vol. 76, no. 11, pp. 980–987, 2006.
- [22] X. Wang, W. Gao, J. Wang, Z. Wu, W. Yan, V. Gevorgian, Y. Zhang, E. Muljadi, M. Kang, M. Hwang, and Y. C. Kang, “Assessment of system frequency support effect of PMSG-WTG using torque-limit-based inertial control,” in *2016 IEEE Energy Conversion Congress and Exposition (ECCE)*, pp. 1–6, IEEE, sep 2016.
- [23] X. Wang, S. Member, W. Gao, S. Member, J. Wang, S. Yan, M. Kang, S. Member, M. Hwang, S. Member, Y. Kang, S. Member, and E. Muljadi, “Inertial Response of Wind Power Plants : A Comparison of Frequency-based Inertial Control and Stepwise Inertial Control,” pp. 0–5, 2016.
- [24] J. Zhu, C. D. Booth, G. P. Adam, A. J. Roscoe, and C. G. Bright, “Inertia emulation control strategy for VSC-HVDC transmission systems,” *IEEE Transactions on Power Systems*, vol. 28, no. 2, pp. 1277–1287, 2013.
- [25] J. C. Hernández, P. G. Bueno, and F. Sanchez-sutil, “Enhanced utility-scale photovoltaic units with frequency support functions and dynamic grid support for transmission systems,” vol. 11, pp. 361–372, 2017.
- [26] J. F. Conroy and R. Watson, “Frequency response capability of full converter wind turbine generators in comparison to conventional generation,” *IEEE Transactions on Power Systems*, vol. 23, no. 2, pp. 649–656, 2008.
- [27] F. Gonzalez-Longatt, A. Bonfiglio, R. Procopio, and D. Bogdanov, “Practical limit of synthetic inertia in full converter wind turbine generators: Simulation approach,” in *2016 19th International Symposium on Electrical Apparatus and Technologies, SIENA 2016*, 2016.
- [28] T. Ackermann, *Wind Power in Power Systems Wind Power in Power Systems Edited by*, vol. 8. 2005.
- [29] S. Heier, *Grid Integration of Wind Energy*. 3 ed., 1998.
- [30] Q. Wang and L. Chang, “An Intelligent Maximum Power Extraction Algorithm for Inverter-Based Variable SpeedWind Turbine Systems,” *IEEE Transactions on Power Electronics*, vol. 19, no. 5, pp. 1242–1249, 2004.

- [31] M. Barakati, M. Kazerani, and D. Aplevich, “Maximum Power Tracking Control for a Wind Turbine System Including a Matrix,” vol. 24, no. Mc, p. 4244, 2009.
- [32] T. Thriringer and J. Linders, “Control by Variable Rotor Speed of a Fixed Pitch Wind,” *IEEE Transactions on Energy*, vol. 8, no. 3, pp. 520–526, 1993.
- [33] S. M. Barakati, *Modeling and Controller Design of a Wind Energy Conversion System Including a Matrix Converter*. PhD thesis, University of Waterloo, 2008.
- [34] W. Lu and B. T. Ooi, “Multiterminal LVDC system for optimal acquisition of power in wind-farm using induction generators,” *IEEE Transactions on Power Electronics*, vol. 17, no. 4, pp. 558–563, 2002.
- [35] Q. Zeng, L. Chang, and R. Shao, “Fuzzy-logic-based maximum power point tracking strategy for PMSG variable-speed wind turbine generation systems,” *Canadian Conference on Electrical and Computer Engineering*, no. 1, pp. 405–409, 2008.
- [36] W. M. Lin, C. M. Hong, and C. H. Chen, “Neural-network-based MPPT control of a stand-alone hybrid power generation system,” *IEEE Transactions on Power Electronics*, vol. 26, no. 12, pp. 3571–3581, 2011.
- [37] H. Polinder, J. A. Ferreira, B. B. Jensen, A. B. Abrahamsen, K. Atallah, and R. a. McMahon, “Trends in Wind Turbine Generator Systems,” *IEEE Journal of Emerging and Selected Topics in Power Electronics*, vol. 1, no. 3, pp. 174–185, 2013.
- [38] Z. Chen, J. M. Guerrero, F. Blaabjerg, and S. Member, “A Review of the State of the Art of Power Electronics for Wind Turbines,” *IEEE Transactions on Power Electronics*, vol. 24, no. 8, pp. 1859–1875, 2009.
- [39] M. P. Kazmierkowski, R. Krishnan, and F. Blaabjerg, *Control in Power Electronics—Selected Problems*. New York: Academic, 2002.
- [40] F. Blaabjerg, R. Teodorescu, M. Liserre, and A. V. Timbus, “Overview of control and grid synchronization for distributed power generation systems,” *IEEE Transactions on Industrial Electronics*, vol. 53, no. 5, pp. 1398–1409, 2006.

- [41] M. Chinchilla, S. Arnaltes, and J. C. Burgos, “Control of permanent-magnet generators applied to variable-speed wind-energy systems connected to the grid,” *IEEE Transactions on Energy Conversion*, vol. 21, no. 1, pp. 130–135, 2006.
- [42] T. Orłowska-Kowalska, F. Blaabjerg, and J. Rodríguez, *Advanced and intelligent control in power electronics and drives*. 2014.
- [43] H. Brantsæter, Ł. Kocewiak, A. R. Årdal, and E. Tedeschi, *Passive filter design and offshore wind turbine modelling for system level harmonic studies*, vol. 80. Elsevier B.V., 2015.
- [44] F. M. Gonzalez-longatt, “Activation Schemes of Synthetic Inertia Controller on Full Converter Wind Turbine (Type 4),” no. Type 4, 2015.
- [45] S. Papathanassiou, “Models for Variable Speed Wind Turbines,” p. 1997.

Appendix A

WIND TURBINE PARAMETERS

Property	Value	Unit
Turbine Type	GE2.75-103	-
Rated Turbine Power	2.75	MW
Converter Power Rating	3.04	MVA
Rotor Diameter	103	m
Blade Inertia	12600000	kgm^2
Generator Speed Range	550-1735	rpm
Rotor Speed Range	4.7-14.8	rpm
Cut-in Wind Speed	3	m/s
Cut-off Wind Speed	25	m/s
Air Density	1.225	kg/m^3
Gearbox Ratio	117.4	-
Generator Rated Voltage	690	V
Generator Type	PM Synchronous	-
Generator Inertia	240	kgm^2
Generator Pole	4	-
Generator Flux Linkage	2.5	Vs
DC-Link Capacitance	27	mF
DC-Link Voltage	1200	V

Table A.1: Wind Turbine Parameters Used in the Thesis

Appendix B

P.M. ANDERSON TEST CASE PROPERTIES

Loads	Location (Bus Number)	Active Power (MW)	Reactive Power (MVAr)
Load A	5	125	50
Load B	6	90	30
Load C	8	100	35

Table B.1: Load Data of the P.M. Anderson Test System

From Bus	To Bus	Resistance (R) (pu)	Reactance (X) (pu)	Susceptance (B/2) (pu)
4	5	0.0100	0.8500	0.0880
4	6	0.0170	0.0920	0.0790
5	7	0.0320	0.1610	0.1530
6	9	0.0390	0.1700	0.1790
7	8	0.0085	0.0720	0.0745
8	9	0.0119	0.1008	0.1045

Table B.2: Line Data of the P.M. Anderson Test System

Parameter	Location	Active Power	Reactive Power
	(Bus Number)	(MW)	(MVAr)
Nominal Apparent Power (MVA)	247.5	192	128
Nominal Voltage (kV)	16.5	18	13.8
Nominal Power Factor	1	0.85	0.85
Plant Type	hydro	steam	steam
Rotor Type	salient	round	round
Nominal Speed (rpm)	180	3600	3600
x_d (pu)	0.146	0.8958	1.3125
x'_d (pu)	0.0608	0.1198	0.1813
x_q (pu)	0.0969	0.8645	1.2578
x'_q (pu)	0.0969	0.1969	0.25
x_l (pu)	0.0336	0.0521	0.0742
τ'_{d0} (s)	8.96	6	5.89
τ'_{q0} (s)	0	0.535	0.6
Stored Energy at nominal speed (MWs)	2364	640	301
Inertia (s)	9.5515	3.3333	2.3516

Table B.3: Generator Data of the P.M. Anderson Test System

Transformers	From Bus	To Bus	High Voltage Side	Low Voltage Side	Reactance
			(kV)	(kV)	(pu)
Transformer 1	1	4	230	16.5	0.0576
Transformer 1	2	7	230	18	0.0625
Transformer 1	3	9	230	13.8	0.0586

Table B.4: Transformer Data of the P.M. Anderson Test System